The microtubule-associated protein END BINDING1b: functional domain deletions and root responses to mechanical stimuli

by

Vita Lai

B.Sc., Simon Fraser University, 2012

Thesis Submitted in Partial Fulfillment of the
Requirements for the Degree of
Master of Science

in the
Department of Biological Sciences
Faculty of Science

SIMON FRASER UNIVERSITY

Summer 2016

Approval

Name: **Vita Lai**

Degree: **Master of Science (Biological Sciences)**

Title: ***Microtubule associated protein END BINDING 1b: functional domain deletions and root responses to mechanical stimuli***

Examining Committee:

Chair: Dr. John Reynolds
Professor

Dr. Sherryl R. Bisgrove
Senior Supervisor
Associate professor
Department of Biological Sciences

Dr. Zamir K. Punja
Supervisor
Professor
Department of Biological Sciences

Dr. Lisa Craig
Internal Examiner
Associate Professor
Department of Molecular Biology and Biochemistry

Date Defended/Approved: May 16, 2016

Abstract

The microtubule-associated protein EB1b inhibits root responses to mechanical stimulation. The goal of this study was to understand more clearly how EB1b regulates these responses. Loss of EB1b did not alter root elongation rates in response to mechanical cues. However, overexpressing EB1b had an inhibitory effect on root elongation. Mutant *eb1b-1 Arabidopsis* plants expressing truncated EB1b proteins, with and without GFP fusions, were generated. Truncations included both N-terminal (microtubule-binding) and C-terminal (protein-interaction) domains. Transgenic mutants expressing a truncated version of EB1b missing part of the C-terminal domain were analyzed. The responses of these mutant roots to mechanical stimulation was similar to untransformed *eb1b-1* mutants. Since previous analyses have shown that responses of mutants expressing full-length EB1b are equivalent to wild type, this result indicates that the EB1b C-terminus is required for normal regulation of root responses to mechanical cues and that interactions between EB1b and other, non-tubulin proteins is involved.

Keywords: EB1; *Arabidopsis*; deletion mutant; mechanical stimulation; root growth; Gateway cloning

Acknowledgements

First and foremost, I would like to express my deepest gratitude to my senior supervisor, Dr. Sherryl Bisgrove. I met Sherryl when I took an undergraduate research course with her in the fall term of 2011. One year later, I began my graduate studies in her laboratory. I appreciate her for giving me the freedom to work on my own, while at the same time always making herself available to me whenever I needed help. I thank her for providing valuable input towards my project and thesis, as well as a vibrant environment for learning and doing research. Thanks to Sherryl, I will always remember to ask myself “What is the question?” in my career in research.

In addition to Dr. Bisgrove, I would like to thank Dr. Zamir Punja for being on my supervisory committee, and for taking the time to review my thesis. I would also like to thank Dr. Jim Mattsson, and his lab members, for sharing their laboratory resources with me, and for offering their advice on my work. Without their precious time and support, it would not have been possible to complete this research.

Hae Ryoung (Tommy) Kim provided assistance in screening the transformed plants, and I thank him for his help. I would also like to thank former lab members Shannon Squires and Saeid Shahidi for their friendship, and their contributions - either directly or indirectly - toward my research. Thanks also to Sachini Ariyaratne, and the many other undergraduate students who carried out research projects in our lab. All of these people helped to keep me sane, and entertained, at times when things would get stressful in the laboratory. We shared many frustrating moments (when, after many attempts, assays still would not work), and many exciting moments as well (sometimes, even in getting the littlest things to work out)!

I would like to thank Dr. Moussa Diarra, my former co-op supervisor at Agriculture and Agri-Food Canada, who enlightened me with a glance into the world of research that sparked my interest in this field. It was also Moussa who made me realize that graduate school was indeed a possibility for me.

Finally, a very special thanks to Dr. Scott Briscoe, for all of his guidance and advice. It was Scott who first introduced me to a world of Molecular Biology and Genetics that I could understand, and I am grateful for his patience in answering my endless questions throughout both my undergraduate and my graduate studies. From him, I learned that paying attention to details is important, and how to “think” in order to solve problems - skills that have helped me greatly in my research work.

Table of Contents

Approval ii
Abstract iii
Acknowledgements iv
Table of Contents vi
List of Tables viii
List of Figures viii

Chapter 1 Introduction 1
1.1 Plant roots 2
1.1.1 How do roots grow? 2
1.1.2 Microtubules in root growth 3
1.2 Root responses to gravity and mechanical impedance 5
1.2.1 Gravitropism 5
1.2.2 Detection and response to mechanical stimulation 6
1.2.3 END BINDING 1: a microtubule-associated protein 8
1.2.4 Plant EB1 and root responses to gravity/mechanical stimulation 11
1.3 Knockout of gene function and production of transgenic plants 13
1.3.1 *Arabidopsis* as a model for plant research 13
1.3.2 Targeted modification of a gene: overlap extension PCR 14
1.3.3 Visualization of gene product localization using green fluorescent protein 16
1.3.4 Gateway® cloning technology 17
1.3.5 *Agrobacterium* as a natural plant engineer 19
1.3.6 Modification of the Ti plasmid and creation of a binary system 20
1.3.7 *Agrobacterium*-mediated plant transformation 21
1.4 Research objectives 22

Chapter 2 Materials and Methods 23
2.1 Media 23
2.1.1 Bacterial growth 23
2.1.2 Plant transformation 23
2.1.3 Plant growth 23
2.2 Plant material 24
2.3 Plant growth conditions 24
2.4 Bacterial transformations 24
2.4.1 *Escherichia coli* 24
2.4.2 *Agrobacterium tumefaciens* 25
2.5 PCR, electrophoresis, and DNA precipitation 25
2.6 Restriction digests 26
2.7 DNA sequencing 26
2.8 Creation of *EB1b* fragments with truncations 28
2.9 Modification of Gateway® cloning technology and bacterial transformation 29
2.10 *Agrobacterium*-mediated plant transformation 30
2.11 Identification of homozygous transformed plants 31

2.12 Root analyses 31
2.13 Statistical analysis 32

Chapter 3 Results 33
3.1 Design of EB1b deletions 33
3.2 Production of *EB1b* cDNA fragments with C- or N-terminal truncations 35
3.3 Creation of expression vectors carrying truncated *EB1b* inserts using a modified Gateway® cloning system 38
3.4 Production of homozygous transgenic plants expressing EB1b deletion constructs 42
3.5 Responses of roots expressing an EB1b C-terminal truncation to gravitational/transient mechanical stimulation 45
3.6 Root elongation rate in response to mechanical/gravitational stimulation 47

Chapter 4 Discussion 52

Chapter 5 Conclusions and Future Directions 60

References 62
Appendix A 78

List of Tables

Table 2.1 Primers used in PCR amplifications to produce EB1b truncations, in the modified Gateway® cloning protocol, and in DNA sequencing reactions 27

Table 3.1 Isolation of transgenic lines homozygous for single or multiple closely linked transgenes 43

Table 3.2 *Arabidopsis* lines used in experiments carried out for and discussed in this thesis..... 45

List of Figures

Figure 1.1 Organization of microtubule arrays in *Arabidopsis* root cells 4

Figure 1.2 EB1 interacts with microtubules and non-tubulin proteins within cells..... 9

Figure 1.3 Schematic representation of functional domains in the END BINDING 1 protein homodimer..... 9

Figure 1.4 Schematic diagram of overlap extension polymerase chain reaction 15

Figure 1.5 Schematic diagram of Gateway® cloning..... 18

Figure 3.1 Schematic illustration of EB1b deletion constructs 34

Figure 3.2 Schematic illustration of primer designs for generation of EB1b truncations 36

Figure 3.3 Production of *EB1b* cDNA fragments with N- or C-terminal truncations 37

Figure 3.4 Schematic illustration of modified Gateway® cloning protocol..... 39

Figure 3.5 Restriction digests of entry vectors containing *EB1b* inserts..... 40

Figure 3.6 Truncated *EB1b* PCR products with Gateway™-compatible attachment (*att*L) sites..... 41

Figure 3.7 Restriction digests of expression vectors containing two of the *EB1b* truncations..... 42

Figure 3.8 Effects of EB1b C-terminal tail deletion on root responses to mechanical/gravitational stimulation..... 47

Figure 3.9 The level of transient stimulation does not affect overall rates of root elongation 49

Figure 3.10 Root elongation is correlated with the level of constant mechanical impedance 51
Figure 4.1 Proposed interactions between the EB1b protein and other cellular molecules in wild type, *eb1b-1*, and EB1bΔC2 *Arabidopsis* plants 53
Figure 4.2 Model of EB1b action in *Arabidopsis* roots upon transient mechanical stimulation 58

Chapter 1 Introduction

Most life-forms on Earth are supported, either directly or indirectly, by plants. These photosynthetic organisms are primary producers in the food chain, and they also provide fuel, industrial material, and even medicine for humans. Meyer et al. (2012) have estimated that just over 100 terrestrial plant species contribute more than 90% of the world's food supply. According to the Food and Agriculture Organization Corporate Statistical Database, in 2011, the global human consumption of cultivated crop plants increased to an average of more than 80 g/capita/day of dietary energy, from an average of approximately 64 g/capita/day in 1981 (FAOSTAT, 2015a). Despite the increase in the daily dietary energy consumption, the Food and Agriculture Organization of the United Nations (FAOUN) (2014) estimates that between 2012 and 2014, nearly 805 million people were chronically undernourished. In other words, one in nine people on our planet go to bed hungry every night. By 2050, the number of people on Earth is expected to increase from the current 7.3 billion to over 9.5 billion (FAOSTAT, 2015b), and world food demand will surge as a result. To meet such demand, FAOUN (2011) has predicted that world food production must increase by at least 70 percent. Sustainable plant growth and production are needed to accommodate the energy and nutritional demands of our growing population. Yet both land and water resources for food production are limited, and are already under heavy stresses.

Environmental stresses play crucial roles in the productivity, survival, and development of plants. Plants are subject to many forms of environmental stresses that largely fall into one of two categories: abiotic or biotic. Abiotic stresses include drought, extreme temperatures, heavy metals, and mechanical stresses, while examples of biotic stresses are herbivory, disease, and allelopathy from other plants. As sessile organisms, plant species have adapted unique strategies to cope with these environmental stresses. Stress responses occur in all plant organs, including the roots. Plant root systems are known to display a high degree of plasticity as they develop, in response to the many stressors they encounter in the soil.

1.1 Plant roots

Roots have important roles for plant survival; these structures are essential for anchorage and absorption of both water and nutrients. To accomplish these roles, roots need to be able to penetrate through the soil and direct their growth towards locations where water and nutrient supplies are optimal. Thus, root development is highly receptive to environmental stimuli. As they grow, roots are constantly encountering various environmental stresses and cues, and as a result, modify their developmental activities. A few examples of such modifications include the development of lateral roots in response to mechanical stimulation (Ditengou et al., 2008), the development of root hairs in low phosphorous conditions (Bates and Lynch, 1996), and directional changes in root growth to avoid saline environments (Galvan-Ampudia et al., 2013). Directional root growth is a type of tropic response in which roots reorient their growth path in reaction to stimuli. Such phenomena indicate that roots must have mechanisms that allow them to "read" complex environmental conditions, and respond by navigating toward beneficial cues and away from harmful ones. Understanding how roots grow and accomplish such navigational feats are important steps in addressing the immediate issues facing our growing population, from food security to human nutrition. The ability to design plants with improved root systems will achieve potentially both greater overall productivity and growth, even in some regions of the world where growth is not possible now.

1.1.1 How do roots grow?

During root growth, plants control patterns of cell division and cell expansion. Cell division occurs in an area of the developing root known as the meristem. The newly generated cells are small and grow slowly in both length and breadth. As they enter the transition zone, cellular activities are reoriented from those necessary for cell division to those required for cell expansion. During the process of cell expansion, cell volume is augmented by increasing the turgor pressure inside of the cell via the uptake of water into the central vacuole. Normally, cross-linkages of cellulose microfibrils to a matrix of hemicellulose provide cell walls with sufficient tensile strength to withstand such turgor-driven forces. However, during cell expansion, disruption in the polysaccharide cross-linkages across the entire cell surface loosens the cell wall, resulting in a rapid isotropic

enlargement of the cell. This modification of the polysaccharide network is accomplished by the acid activation of enzymes located in the cell wall, and is regulated by the phytohormone auxin (Rayle and Cleland, 1992). As the expanding cell enters the elongation zone, expansion becomes restricted to the sides of the cell that are parallel to the long axis of the root. As such, cell length increases dramatically compared to cell width during this elongation process, leading to a long and narrow root. Regulating the orientation of cell expansion is critical to the direction of root growth, and microtubules have been found to play vital roles in this process (Ishida and Hashimoto, 2007; Furutani et al., 2000; Thitamadee et al., 2002; Galva et al., 2014).

1.1.2 Microtubules in root growth

Microtubules are components of the cytoskeleton that form via the polymerization of α- and β-tubulin heterodimers. These tubular cytoskeletal filaments are highly dynamic structures, due to the constant assembly and disassembly of the tubulin dimers at their ends. Such dynamics provide the flexibility to rearrange microtubules into different array patterns within the cell, depending on cellular needs/activities. For example, in dividing root cells, microtubule arrays appear as preprophase bands (to set up the position of the future cell plate) (Pickett-Heaps and Northcote, 1966), as mitotic spindles (to separate the newly divided chromosomes), and as phragmoplasts (to transport materials for construction of the new cell wall) (Staehelin and Hepler, 1996) (Figure 1.1). However, in elongating root cells (i.e., during interphase), microtubules are arranged in parallel hoops, just beneath the plasma membrane, perpendicular to the axis of growth (Ledbetter and Porter, 1963).

Cortical microtubules and cellulose microfibrils are co-aligned in elongating cells. Plants carrying mutations in katanin (a microtubule-severing protein) are found to contain both disorganized cortical microtubules and disorganized cellulose microfibrils (Burk and Ye, 2002). However, Himmelspach et al. (2003) have demonstrated that treatment of roots with the cellulose synthesis inhibitor 2,6-dichlorobenzonitrile reduces the ability of cortical microtubules to form transverse arrays. Taken together, these results illustrate the intimate relationship between these cellular components, each of which seems to play a major role in the organization of the other. As reviewed by Baskin (2001), many models have been put forward to explain the relationship between cortical

microtubules and cellulose microfibrils. The earliest hypothesis, proposed by Green (1962), suggests that cortical microtubules serve as guides for cellulose synthases as they deposit cellulose microfibrils, and thus the pattern of cellulose microfibril arrangement determines the shape of plant cells. However, studies carried out by Baskin et al. (1994), Fisher and Cyr, (1998), Arioli et al. (1998), Whittington et al. (2001), and Burk and Ye (2002) have demonstrated that disrupting the organization of either the microtubules or the cellulose microfibrils, by mutation or pharmacological agents, leads to directional cell expansion defects. Also contrary to the hypothesis put forward by Green, some investigations suggest that microtubule orientation does not always predict the alignment of cellulose microfibrils (Wilms et al., 1990; Sugimoto et al., 2003). These researchers found that cellular cellulose microfibrils were not altered when microtubule organization was disrupted by the microtubule depolymerizing agent oryzalin or the microtubule stabilizing agent taxol.

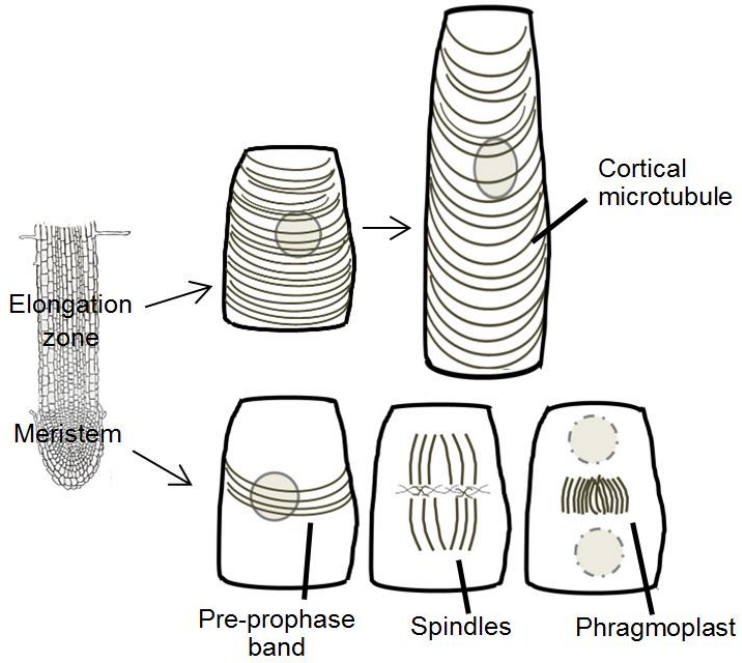

Figure 1.1 Organization of microtubule arrays in *Arabidopsis* root cells

In the meristemic zone, cell division occurs to generate new cells. During cell division, microtubule arrays are arranged as dense ring-like pre-prophase bands (to set up the position of the future cell plate), as mitotic spindles (that segregate the newly divided chromosomes), and as phragmoplasts (to transport materials for construction of the new cell wall). In the elongation zone, cortical microtubules within the cells are located just beneath the plasma membranes and are arranged transverse to the longitudinal direction of cell growth. During cell expansion, cell length increases dramatically compared to cell width, leading to an elongated cell.

1.2 Root responses to gravity and mechanical impedance

The ability of roots to grow through the soil depends not only on turgor-driven cell elongation, but it also relies on effective mechanisms for detecting and responding to the surrounding environment. As soil conditions are not always optimum, root growth can be limited by the physical, chemical, and biological properties of the soil. Gravity and mechanical impedance (soil that is too hard for roots to penetrate efficiently) represent two physical cues that roots are continuously responding to.

When growing in a heterogeneous soil, roots often encounter impenetrable obstacles (Vaughn et al., 2011; Monshausen and Gilroy, 2009). Such obstructions do not necessarily limit growth and development, as roots are able to redirect their growth so that they can wind around such impenetrable objects. The mechanisms that underlie root responses to touch and gravity signals are not yet fully understood. However, it is generally believed that the first step of either response involves the perception of physical cues, which in turn are converted to biochemical signals that lead to modifications in root developmental activities.

1.2.1 Gravitropism

Gravitropism is the oriented growth response of plants in accordance with gravity. Roots are positively gravitropic, growing in a downward direction, parallel to the gravity vector, while shoots are negatively gravitropic (i.e., growing upward). In the root cap, columella cells, with their specialized starch-filled amyloplasts (a.k.a. statoliths), serve as gravity-sensors. The most widely accepted proposal regarding graviperception in roots is the starch-statolith hypothesis (Haberlandt, 1914; Kiss et al., 1996; MacCleery and Kiss, 1999). In a normal downward growing root, starch-laden amyloplasts settle to the bottom of the cell in response to gravity. When the root tip is reoriented such that it is no longer parallel with the gravity vector, amyloplasts settle to the new bottom of the plasma membrane in the cell. This change in amyloplast sedimentation triggers a signaling pathway through the activation of postulated mechanosensitive ion channels which leads to differential cell growth and roots bending downwards (Leitz et al., 2009; Perbal et al., 1997; Stanga et al., 2009). The starch-statolith hypothesis is supported by the gravitropic growth responses of starch-deficient mutants (Kiss et al., 1996). These

mutant plants are either unable to produce starch at all or produce less starch than their wild type counterparts. These researchers found that roots of starchless mutant plants were least responsive to gravity, while the reduced starch mutants displayed an intermediate level of graviresponsiveness.

Given that the starchless mutant retains a residual gravitropic response, one cannot exclude the possibility that plants have other mechanisms for gravity sensing. The gravitational pressure model proposed by Staves (1997) postulates that the cell perceives gravity by sensing the weight of the entire protoplast, not just the intracellular-sedimenting materials. When the gravity-driven protoplast settles upon the cell wall or extracellular matrix, it creates differential pressure between the plasma membrane and the extracellular matrix at the top and the bottom of the cell. These authors propose that this difference in pressure activates putative gravity-sensors located at the top and the bottom of the plasma membrane, triggering graviresponsive events.

Common downstream effects upon activation of the gravity sensors include the transport of gravitropic signals from the root cap to the elongation zone where downward bending of the root occurs. The plant hormone auxin is thought to serve as a carrier for gravity signals. Auxin is produced in the aerial parts of the plant and travels in a pattern like an “inverted fountain”, downward through the central cylinder of a root to the root tip, and then back up to the base of the root through the outer cell layers (Ljung et al., 2001; Swarup et al., 2005). This even distribution of auxin causes the root to grow straight downward. In a gravity stimulated root (i.e., a root that is placed on its side), auxin becomes unequally distributed around the root. More auxin flows through the lower flank of the root, while less auxin flows through the upper flank (Young et al., 1990). This difference in auxin concentration leads to a differential cell expansion rate between the upper and lower flanks, causing the root to bend (Rashotte et al., 2000; Swarup et al., 2005; Mullen et al., 1998).

1.2.2 Detection and response to mechanical stimulation

While it appears that roots are able to sense and respond to mechanical cues, the various molecular mechanisms by which such sensing and responding are accomplished are still largely unknown. The current hypothesis is that mechanical

stimulation/touch is sensed by channels or receptors embedded in the plasma membranes of the root tip cells (Klusener and Weiler, 1999; Massa and Gilroy, 2003). When roots encounter an impenetrable object, the mechanical force causes the plasma membrane and/or cytoskeleton and extracellular matrix to deform, which can relocate or change the conformation of the sensors. This change leads to activation or deactivation of the sensors, triggering the downstream events.

Mechanosensitive ion channels in the plasma membrane are a common mechanism across multiple phyla for perceiving and responding to mechanical forces (see reviews by Monshausen and Haswell (2013) and Hamilton et al. (2015)). Although their activities are quite diverse with regard to selectivity, conductance, and voltage dependence, one common feature is the gating mechanism that has the capability to transduce membrane tension directly into ion flux. Mid1-complementing activity (MCA) is a novel land plant-specific family of membrane-associated proteins that function as calcium-permeable ion channels (Kurusu et al., 2012). The ability of *Arabidopsis* MCA1 to rescue a yeast *mid1* mutant lacking a putative calcium-permeable stretch-activated channel component suggests the function of MCA1 as an integral plasma membrane protein that mediates calcium ion uptake (Nakagawa et al., 2007). *Arabidopsis* plants with mutations in MCA1 have roots that are less able to penetrate a layer of hard agar, further demonstrating the involvement of MCA1 in mechanical responses. Mechanosensitive channels of the small conductance (MscS-like) family, on the other hand, are homologues to MscS in *Escherichia coli*, the organism in which the channel was first identified (Martinac et al., 1987). The bacterial MscS is known for its function as a safety valve to avoid cell rupture by releasing cytoplasmic solutes upon hypoosmotic stress. Whether the plant homologue has a similar role in root responses to mechanical stimulation is still unclear.

In a microarray analysis, Kimbrough et al. (2004) found close to 1700 genes in the *Arabidopsis* root apex that have significant changes in their expression upon mechanical stimulation. The majority of these genes give rise to transcription factors, transporters, and cell wall modifying agents, as well as some proteins of unknown function. The proteins encoded by ninety-six percent of these mechanically-induced genes also play a role in responses to gravity stimulation, suggesting an intricate relationship between plant responses to the two stimuli. A great variety of other genes

are also regulated by stresses, such as drought, cold, and light. Certainly, this finding provides a large number of candidate genes with probable roles in stimuli-specific responses. More detailed mutational analyses can be employed to determine whether these particular genes are necessary for mechanical-sensing and/or -responding, and specifically how they accomplish such tasks.

The gene encoding the microtubule associated protein END BINDING 1 (EB1) is one of the candidate genes found in the Kimbrough et al. (2004) study. Several studies have linked this protein to the regulation of root responses to mechanical and/or gravitational cues (Bisgrove et al., 2008; Squires, 2013; Shahidi, 2013; Gleeson et al., 2012; Squires and Bisgrove, 2013; Galva et al., 2014).

1.2.3 END BINDING 1: a microtubule-associated protein

EB1 is highly conserved among eukaryotic species. It belongs to a group of proteins known as microtubule-associated proteins that preferentially interact with the growing ends of microtubules (Figure 1.2). Although EB1 proteins were the first microtubule plus-end tracking proteins (+TIPs) identified in plants (Chan et al, 2003; Mathur et al., 2003; Gardiner and Marc, 2003; Meagher and Fechheimer, 2003), these proteins were originally discovered as interacting partners of adenomatous polyposis coli (Su et al., 1995), a molecule that has been linked to sporadic and familial forms of colorectal cancers in humans (Miyoshi et al., 1992; Powell et al., 1992). For this reason, much of our knowledge about EB1 has come from studies in yeast and mammalian models (reviewed by Tirnauer and Bierer, 2000; Slep, 2010; Galjart, 2010).

Proteins of the EB1 family contain a conserved N-terminal calponin homology (CH) domain, followed by a variable linker region, and a conserved C-terminal region consisting of an α-helical coiled coil that overlaps with an EB homology domain - the defining feature of the EB1 family (Komaki et al., 2010; Hayashi and Ikura, 2003; Honnappa et al., 2005) (Figure 1.3). The globular calponin homology domain recognizes growing microtubule ends and mediates interactions with microtubules. In the C-terminal region, the coiled coil mediates the parallel homodimerization of EB1 monomers, and the EB homology domain provides binding surfaces for other interacting molecules (Figure 1.2).

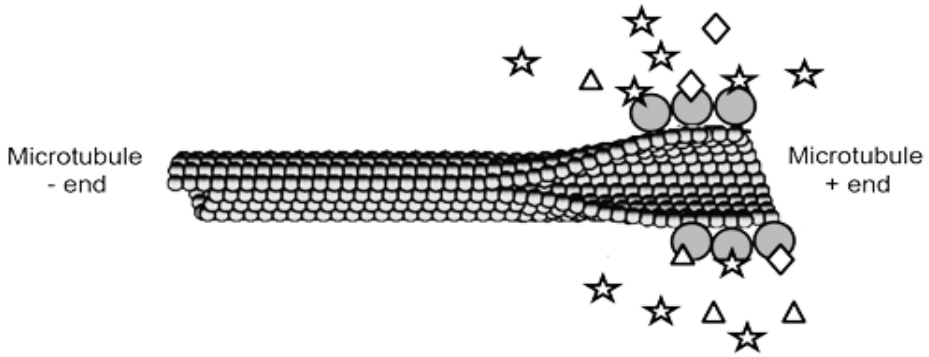

Figure 1.2 EB1 interacts with microtubules and non-tubulin proteins within cells

EB1 proteins (circles) bind to the "+" end of microtubules via their N-terminal calponin homology domain. The EB homology and tail domains at the C-termini of the proteins are involved in the binding of other cellular molecules (stars, diamonds, and triangles).

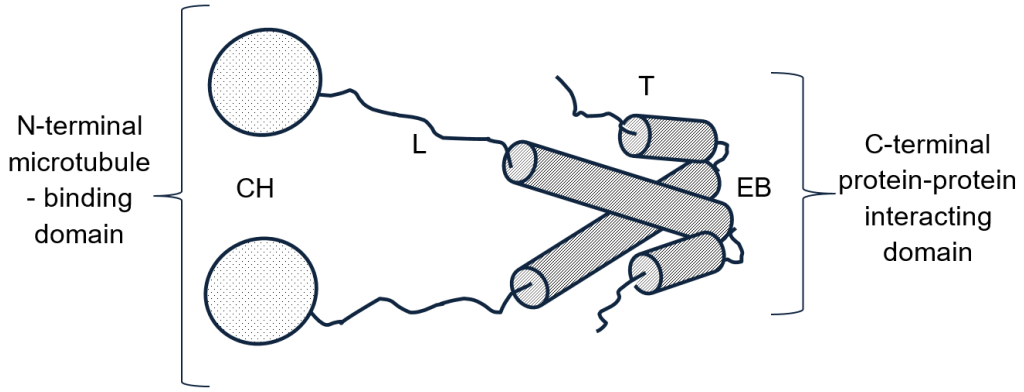

Figure 1.3 Schematic representation of functional domains in the END BINDING 1 protein homodimer

This model shows the structural organization of the homodimeric END BINDING 1 (EB1) protein. Each EB1 protein consists of a conserved, globular, amino terminal calponin homology (CH) domain, a variable linker (L) region, a conserved C-terminal domain including a coiled-coil that overlaps with the end binding (EB) homology domain, and a tail (T) region. The N-terminal CH domain is responsible for the microtubule plus-end tracking ability. The coiled-coil region of the C-terminal domain controls the dimerization of EB1 monomers, while the EB homology region provides interacting surfaces for other proteins.

Time-lapse microscopy of live mammalian cells at interphase shows that protein fusions of GFP to EB1 are found specifically associated with the dynamically growing ends of microtubules (Mimori-Kiyosue et al., 2000). It is not known exactly to what extent EB1 binds the tubulin subunits. However, it has been shown that as "new" tubulin dimers

are added on to the growing plus-ends of microtubules, EB1 bound to the “older” tubulin subunits within the microtubules are released. Thus, the apparent movement of EB1 in time-lapse movies presents as comets (Mimori-Kiyosue et al., 2000). However, EB1 does not translocate or “surf” along microtubules in the same way that kinesin motor proteins typically do.

Because EB1 has the ability to bind microtubules, researchers have studied changes in microtubule behaviour that occur upon interaction with EB1 (Van Damme et al., 2004; Bisgrove et al., 2008; Komaki et al., 2010; Manna et al., 2008; Vitre et al., 2008; Coquelle et al., 2009; Komarova et al., 2009). While all of these investigators found that EB1 can influence microtubule dynamics, the effects of EB1 binding on microtubule growth and shrinkage were anything but “clear cut”, and varied with the cell type studied, the specific EB1 proteins used, their concentrations, and the presence or absence of other +TIPs.

In a 2012 proteomic study, Jiang et al. demonstrate that many +TIPs, signaling molecules, and cytoskeletal-associated proteins have the potential to interact with mammalian EB1. It has been suggested that EB1 serves as a hub for the recruitment of these proteins to microtubule plus ends (Vaughan, 2005; Lansbergen and Akhmanova, 2006). In animal cell migration studies, EB1 has been shown to regulate actin and microtubule remodeling activities by recruiting cell motility factors to microtubule ends (Schober et al., 2009). In budding yeast, it has been revealed that microtubule ends can indirectly interact with actin-based motor components through EB1, allowing microtubule ends to travel along actin filaments during mitotic spindle positioning (Liakopoulos et al., 2003).

Rogers et al. (2004) have demonstrated that signaling molecules, like the cellular shape regulator (a rho-type guanine nucleotide exchange factor), were delivered to target sites in the cell cortex of *Drosophila melanogaster* through association with EB1 at the microtubule ends. Similarly, in axonal targeting, the successful transportation of voltage-gated potassium channels relies on their interaction with EB1 on the microtubule ends (Gu et al., 2006). As suggested by Bisgrove (2011), the role of EB1 may be to either concentrate its interacting partners in the vicinity of other components of the signaling pathway or to sequester them away from their signaling partners.

1.2.4 Plant EB1 and root responses to gravity/mechanical stimulation

The *Arabidopsis thaliana* genome contains three EB1 genes: *EB1a* (At3g47690), *EB1b* (At5g62500), and *EB1c* (At5g67270) (Bisgrove et al., 2004; Gardiner and Marc, 2003). Both EB1a and EB1b track the growing plus ends of microtubules in mitotic and elongating interphase cells. EB1c, on the other hand, is sequestered in the nucleus during interphase, but is localized to microtubule ends during mitosis (Dixit et al., 2006; Komaki et al., 2010; Chan et al., 2003; Mathur et al., 2003; Van Damme et al., 2004; Bisgrove et al., 2008).

To study the mechanisms that mediate root responses to a combination of mechanical and gravitational signals, mutant seedlings are often grown on the surface of reclined agar plates (Okada and Shimura, 1990). Normally, roots grow downward in response to gravity. However, when root tips encounter the agar surface, they find it impenetrable (given the concentration of agar used in making the plates), and redirect their path of growth in attempt to maneuver around the object. The force builds as the elongating cells continue to push the root tip against the agar. When sufficient force exists and the root tip is not able to push through the agar surface, the root bends at the base of the elongation zone. The elongating cells continue to expand until the root eventually buckles. This buckling of the root causes the root tip to be displaced from the downward orientation of growth, triggering a gravitropic response. This response results in a differential growth rate in the elongating cells across the root. As a result, another bend forms, allowing the root tip to reorient back to the downward direction of growth. This regime repeats as the root grows downward and once again encounters the agar surface. These repeating responses to transient stimulation cause roots to skew off to one side as they grow. Under such growing conditions, roots perceive and respond to a combination of mechanical and gravity cues. Thus, roots adopt a wavy pattern of growth and deviate from the strictly downward direction of growth.

In one study, the phenotypes resulting from the disruption of each of the three *EB1* genes – singly, as well as in double and triple mutant combinations – were characterized for their ability to respond to mechanical and/or gravitational stimuli (Bisgrove et al., 2008). Seedlings of these mutants grown on the surface of agar plates

reclined from a vertical orientation have roots that tend to form loops and deviate more from a downward growth trajectory than wild type. These observations suggest that EB1 has an inhibitory effect on root responses to mechanical/grvitational cues. However, all three of these mutants do not respond equally. Of the three *EB1* genes, plants expressing mutated forms of *EB1b* show the most severe defects in root responses to combinations of gravity and touch stimuli, suggesting that *EB1b* plays a larger role in root responses to touch/gravity signals than either *EB1a* or *EB1c*.

Another recent study demonstrated that transgenic *eb1b-1* mutants that over-express *EB1b* develop roots with less deviation from a downward growth trajectory and fewer loops than wild type roots. In the same study, transgenic *eb1b-1* mutants that express *EB1b* at the wild type level were shown to have similar root skewing angles and a similar amount of root loops as the wild type plants (Squires et al., manuscript in preparation). These observations suggest not only that EB1b has an inhibitory effect on root responses to mechanical and gravitational cues, but also that the amount of repression correlates with the level of *EB1b* expression. Although EB1b activities have been linked to the regulation of microtubule dynamics, membrane trafficking, and interactions with various other proteins, including members of signaling pathways and other +TIPs (Rogers et al., 2004; Galva et al., 2014; Shahidi, 2013), it is not known exactly how EB1b contributes to the regulation of root responses to these cues.

In this thesis, I examine the molecular mechanisms of EB1b by which roots respond to combinations of mechanical and gravity stimulation. To gain insight as to how EB1b is involved in these responses, root behavior of plants carrying EB1b mutations are analyzed. The generation of these EB1b mutant plants constitutes a main component of my thesis. The process of producing the mutant plants includes the design and production of the EB1b truncation constructs, cloning of the constructs, plant transformation with the cloned constructs, and screening of the resulting plants. Following production of the mutant plants, root analyses are performed. In section 1.3, I discuss the background of some of the methodology used to produce the transgenic plants for my study.

1.3 Knockout of gene function and production of transgenic plants

One of the classical approaches to investigate the function of a gene is to analyze the phenotypes of organisms carrying mutations within that gene. The ultimate goal of this approach is to understand the function(s) of the gene product more completely (i.e., not just what the gene product is and does, but how it goes about doing it). The development of Sanger DNA sequencing in the 1970s (Sanger et al., 1977) followed by the polymerase chain reaction (PCR) in the 1980s (Mullis et al., 1986) sparked the generation of many more molecular tools. Technological advances in cellular and molecular biology have greatly accelerated our understanding of the impact of genetic variation. For example, gene products can be fused to tags that can be used to visualize their location and movement within cells.

In this section, I describe selected strategies used to generate transgenic *Arabidopsis* plants that carry specific mutations within a specific gene. I also describe how to grow such transformed plants in an artificial setting to study root responses to mechanical and gravitational stimuli. The workflow usually starts with manipulating the DNA sequence of the gene of interest, and cloning the modified version of the gene into a vector *in vitro*, followed by introduction of the vector into the lab workhorse *Escherichia coli* for propagation, and then into the natural plant engineer *Agrobacterium* to incorporate the mutated gene into the plant genome. After screening the transgenic plants thus produced, root behavior can be studied as plants are grown in an agar medium that provides mechanical stimulation in a controlled environment.

1.3.1 *Arabidopsis* as a model for plant research

Arabidopsis is a member of the mustard (Brassicaceae) family, which also includes such common plants as radish, turnip, cauliflower, and cabbage. *Arabidopsis* itself is not of major agronomic significance. In fact, it's quite the opposite; *Arabidopsis* is considered as a weed. However, Meyerowitz (1989) describes *Arabidopsis* as a "useful weed", as it offers important advantages for plant research. Characteristics such as small size, short generation time (as short as 6 weeks), the ability to self-pollinate, and to generate large quantities of seeds are some of the reasons for *Arabidopsis* being widely

used as a model for crop plants (Koornneef and Meinke, 2010). In addition to these advantages, *A. thaliana* is the first plant for which the complete genome has been sequenced (The *Arabidopsis* Genome Initiative, 2000). A fully annotated genome sequence has been developed and is constantly being updated for this organism (Huala et al., 2001). As a result, *Arabidopsis* has become an important research model for the attainment of both fundamental knowledge of plant-specific research and comprehensive comparisons of conserved processes in other eukaryotes (Reddy and Day, 2001; Riechmann et al., 2000). The implications of such studies are relevant not only for basic plant research, but also can be applied to other fields of research, including agricultural sciences and molecular medicine (Obembe et al., 2011; Fischer and Emans, 2000).

1.3.2 Targeted modification of a gene: overlap extension PCR

There are many ways to induce a mutation in a targeted gene, from the more traditional method of cleaving the DNA strands with restriction endonucleases (Smith and Welcox, 1970; Loenen et al., 2013) to the more sophisticated method of exchanging DNA sequences through homologous recombination (Hutchison et al., 1978; Beetham et al., 1999; Kempin et al., 1997). An alternative method is the use of overlap extension PCR, which allows the creation of a chimeric gene from the fusion of selected PCR-amplified DNA fragments (Higuchi et al., 1988). Because of its sensitivity and specificity, PCR is able to amplify a particular DNA sequence from a targeted gene *in vitro* (Mullis et al., 1986). For this reason, the PCR technique has become a staple for many applications in biological research and for early diagnostics in multiple areas of medicine and infectious disease (Hagelberg, 1991; Bermingham and Luettich, 2003; National Laboratory of Enteric Pathogens, 1991).

The method of overlap extension PCR is similar to conventional PCR. Both approaches are based on the idea that primers designed to anneal to targeted DNA sequences can be extended by DNA polymerase. However, the primers in the overlap extension PCR generate DNA products that consist of “overlapping ends” that are complementary to the junctions of the adjacent DNA fragments (Wurch et al., 1998; Ge and Rudolph, 1997) (Figure 1.4). These overlapping ends allow the two desired DNA fragments to recognize one another at one extreme end during PCR. The chimeric PCR product is then produced in the second set of PCR reactions, where one of the DNA

strands from each of the first PCR products now serves as both PCR template and primer. Using this approach, not only can the sequence of a gene can be modified specifically through reconstructing the nucleotide sequence, but also genes can be readily fused with things like epitope tags, localization signals, secretory sequences, and/or proteolytic signals. Furthermore, sequences required for the binding of DNA or other functional elements also can be inserted into proteins of interest in this manner (Mehta and Singh, 1999).

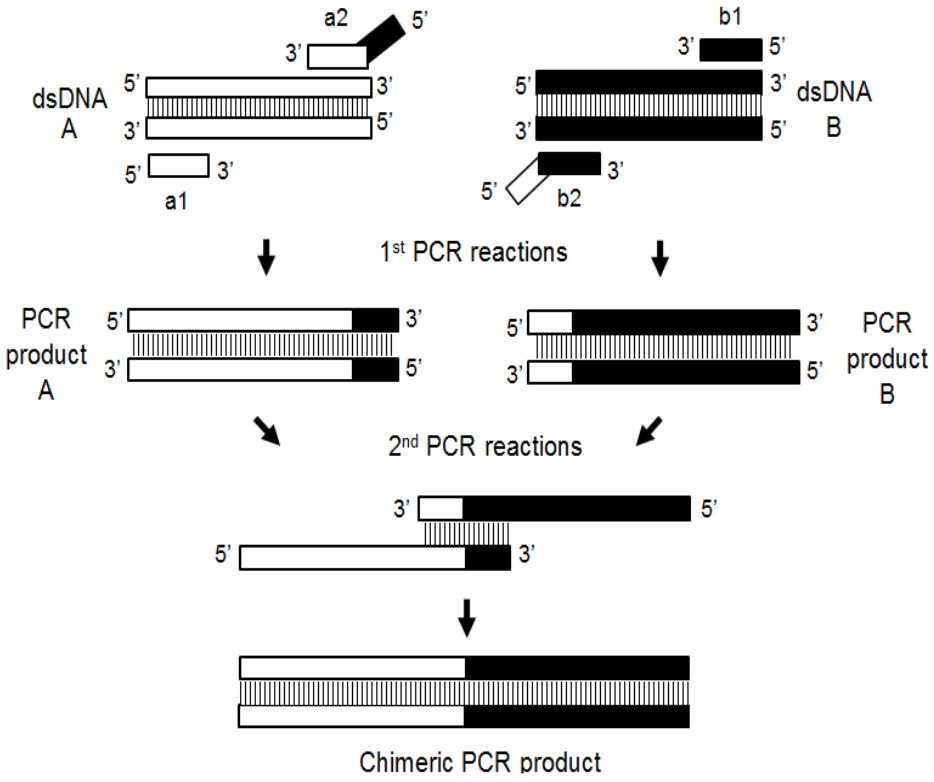

Figure 1.4 Schematic diagram of overlap extension polymerase chain reaction

Overlap extension PCR involves the generation of chimeric DNA fragments by connecting individual DNA fragments. Double stranded (ds) DNA fragments A (white bars) and B (black bars) are amplified in independent PCR reactions, each with their own set of primers (a set of primers is shown as a1 and a2, or b1 and b2). One primer from each set (a2 and b2) contains an extended sequence that is complementary to the junction of the other DNA fragment. After the first set of PCR reactions, a section of PCR products A and B is identical. The chimeric gene is generated in the second set of PCR reactions, where one of the DNA strands from each of the first PCR products now serves as both PCR template and primer.

1.3.3 Visualization of gene product localization using green fluorescent protein

In cellular biology, the study of protein localization in transgenic cells and tissues is of common interest. These analyses can be accomplished through translational fusion of photon-emitting tags like green fluorescent protein (GFP) to a protein of interest. Overlap extension PCR, as described in section 1.3.2, would be one method of use for the production of such translational fusions.

Discovered by Shimomura et al. in 1962, GFP is a naturally fluorescent molecule isolated from the jelly fish *Aequoria victoria*. Since its discovery, GFP has been utilized in studies of the subcellular properties and localization of a great variety of proteins. The critical breakthrough came with the cloning and expression of the DNA encoding GFP in cells of organisms other than *A. victoria*, such as *Escherichia coli* (Prasher et al., 1992) and *Caenorhabditis elegans* (Chalfie et al., 1994; Inouye and Tsuji, 1994). Unlike luciferase (another photon-producing protein commonly used for such purposes), exogenous substrates and cofactors are not required for GFP to exhibit fluorescence. Spectral variants, including blue, cyan, and yellow fluorescent proteins also have been created by modification of the GFP coding sequence (as summarized in Muller-Taubenberger and Anderson, 2007). Along with the *Discosoma* coral-derived red fluorescent protein (Matz et al., 1999), these fluorescent variants can serve as spectrally distinct companions or can substitute for GFP. Like GFP, they are also widely used in both transcriptional fusions (as genetically encoded indicators of gene expression) and translational fusions (to monitor protein/cellular localization) (Stewart, 2001; Chalfie et al., 1994; Gerdes and Kaether, 1996).

The translational fusion of GFP as a tag is typically attempted at either the amino or carboxyl terminus of the protein under study, sometimes with intervening spacer peptides. This approach offers live-cell imaging that allows researchers to follow individual cells and take pictures at frequent intervals during the incubation period, making it possible to get a time-lapse of the cellular localization/activities of a protein. Because fixation processes (involving formaldehyde, ethanol, or other strong treatments) are not used, the transgenic cells and tissues remain alive during GFP visualization, thereby also avoiding the possible introduction of artifacts (due to cellular fixation) before

microscopic viewing. In the ideal condition, fusion of the GFP tag does not interfere with the normal function and localization of the host protein in the living cells, although this is not always the case (Skube et al., 2010; Prescott et al., 1999). Despite this shortfall, GFP fusion tagging remains a popular choice for cellular imaging, and has been used successfully in many organisms, ranging from viruses (Ward and Moss, 2001) to *Xenopus* (Jin et al., 2003) to plants (von Arnim et al., 1998) to mammals (Gillooly et al., 2000).

1.3.4 Gateway® cloning technology

Once the modified version of a gene of interest is created, it is ready to enter the "Gateway". Gateway® cloning technology is a universal cloning method that relies on site-specific recombination mediated by enzymes derived from bacteriophage lambda (Landy, 1989). There are two general steps involved in the Gateway® cloning procedure (Figure 1.5). The initial step involves inserting the DNA fragment of interest into donor vectors by homologous recombination, to produce entry vectors. The second step involves homologous recombination between the entry vectors and the application-specific destination vectors to produce expression vectors, which are then carried forward for specific downstream analyses. After each step of this Gateway® process, bacterial cells (in most cases, *Escherichia coli*) are transformed with the recombinant products for selection and amplification purposes.

One of the advantages of using Gateway® cloning technology is the selection system used to identify recombinants. Gateway® vectors consist of at least one species-specific bacterial origin of replication, and two selective markers: a suicide gene located between the recombination sites (named the attachment sites), and an antibiotic resistance gene within the vector backbone. During homologous recombination, the suicide gene and the DNA fragment of interest are exchanged between the two interacting vectors. Only bacterial cells that acquire the recombinant products carrying the antibiotic resistance gene, without the presence of the suicide gene, are able to survive. As a result of these two forms of selection, high levels of positive clones are obtained following transformation into an appropriate *E. coli* strain.

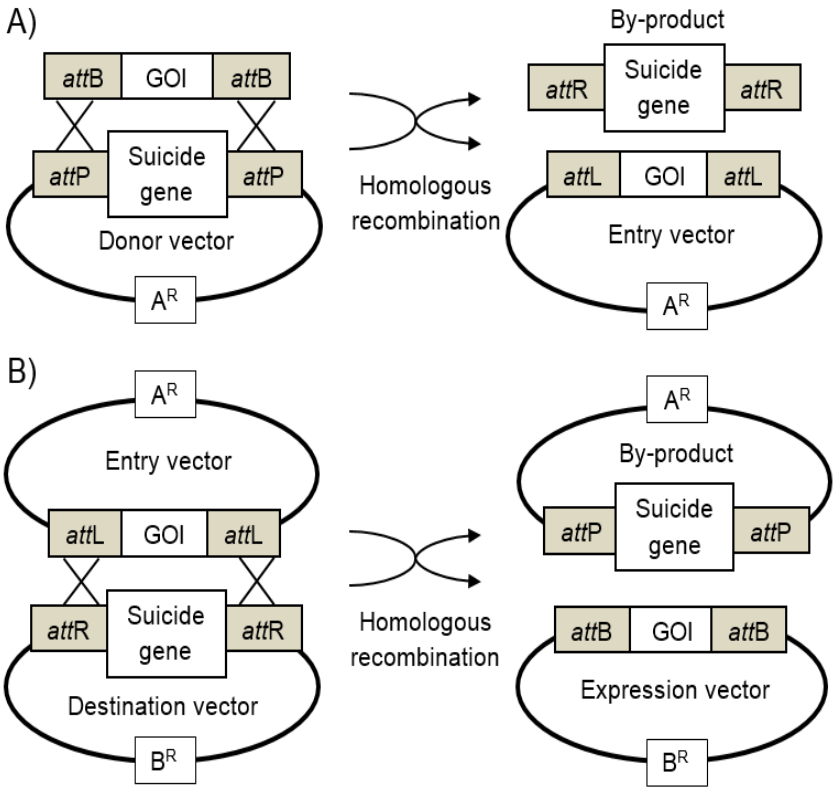

Figure 1.5 Schematic diagram of Gateway® cloning

Gateway® cloning relies on homologous recombination at the attachement (*att*) sites to exchange DNA fragments between the two interacting nucleic acid molecules. (A) The gene of interest (GOI) is first inserted into a donor vector by homologous recombination occuring between the *att*P and *att*B sites, to produce entry vectors. Bacterial cells that undergo successful transformation are selected based on resistance to antibitoic A (encoded by the A^R gene). (B) Homologous recombination between the selected entry vectors and the application-specific destination vectors takes place to produce expression vectors. Genes located between the *att*L and *att*R sites are exchanged between these two interacting vectors. Bacterial cells carrying expression vectors (containing the GOI, and lacking the suicide gene) are selected for, as they will be the only bacteria able to grow in the prescence of antibiotic B. Clones containing the expression vectors are then carried forward to the specific downstream application of interest.

The choice of destination vectors is usually organism- and application-specific. For example, for the purposes of *Agrobacterium*-mediated plant transformation, the organism-specific destination vector would carry sequences that *Agrobacterium* strains need to accomplish plant transformation. If subcellular localization of a protein is of interest in the research, an application-specific destination vector containing the DNA sequence of a fluorescent molecule (such as the green florescent protein) in-frame with the gene of interest would also be needed. Since the creation of Gateway® cloning, a

number of laboratories have customized destination vectors to contain genetic elements of use in their specific studies. For example, Curtis and Grossniklaus (2003) have inserted cauliflower mosaic virus 35S-derived promoters into their destination vectors, for the study of constitutive ectopic gene expression in plants. Such developments have made cloning preparations more efficient for studying functional analyses and protein expression, not only in plants (Himmelbach et al., 2007; Curtis and Grossniklaus, 2003; Gehl et al., 2009; Brand et al., 2006; Earley et al., 2006), but also in other organisms (Frandsen, 2011; Akbari et al., 2009; Nyabi et al., 2009; Alberti et al., 2007; Roure et al., 2007).

1.3.5 *Agrobacterium* as a natural plant engineer

Agrobacterium are bacteria that naturally inhabit the soil, where they commonly occur in the rhizosphere and survive primarily on decaying organic matter (Escobar and Dandekar, 2003). Among *Agrobacterium* species, *A. tumefaciens*, previously known as *Bacterium tumefaciens* (Smith and Townsend, 1907), has the ability to cause crown gall disease in over 90 plant families, including Brassicaceae (De Cleene and De Ley, 1976). As the name suggests, this disease is characterized by the formation of tumours on the affected plant tissues. Schilperoort et al. (1967) demonstrated that *Agrobacterium* DNA was found within a DNA extract of plant crown galls, spawning the possibility of genetic engineering in plants. Prior to this finding, the notion of *Agrobacterium* genes (or any other foreign genes, for that matter) integrated into a plant genome and functioning in a plant cell seemed rather far-fetched.

In 1947, Braun proposed that *A. tumefaciens* transferred and expressed its “tumour-inducing principle” into plant hosts, causing the plant cells to proliferate uncontrollably. This so-called “tumour-inducing principle” was later identified as transfer DNA (T-DNA) (Chilton et al., 1977). In general, T-DNA encodes two sets of genes: oncogenes and opine-related genes. The oncogenes encode enzymes that catalyze the synthesis of plant hormones and alter the responsiveness of plants to these hormones (Zhu et al., 2000), ultimately leading to tumour formation. The opine-related genes in T-DNA encode molecules involved in the synthesis of opines: low-molecular-weight amino acid and sugar phosphate derivatives that are produced by infected plants (Dessaux et al., 1986). The activation of these two sets of genes results in abnormal plant cell

proliferation and synthesis of carbon and nitrogen sources that are used by *A. tumefaciens.* A specific type of opines can only be utilized by a specific *Agrobacterium* strain, which creates a selective advantage for that bacterial strain in the crown gall tumour (Kim et al., 2001).

The T-DNA region in *Agrobacterium* is found between two highly homologous 25-28 base pair (bp) direct repeats, named left and right T-DNA borders, on the tumour-inducing (Ti) plasmid (Zaenen et al., 1974; Yadav et al., 1982; Wang et al., 1984). This region becomes a mobile genetic element when the two borders are recognized by the *Agrobacterium* DNA transfer machinery, which initiates the excision of a single-strand of the T-DNA within the border region. The process of transporting and integrating this single strand of T-DNA into the plant genome is controlled by virulence genes carried on the Ti plasmid (Valentine, 2003; Zupan et al., 2000; Pitzschke and Hirt, 2010). Other than the T-DNA transporting machinery, the Ti plasmid also encodes enzymes for the uptake and catabolism of opines (Kim and Farrand, 1996; Lyi et al., 1999; von Lintig et al., 1994). Given its natural ability to infect plants and integrate its DNA into plant genomes, *Agrobacterium* has become a popular model for bacterial pathogenesis, as well as a gene vector for modern plant biology and agricultural biotechnology.

1.3.6 Modification of the Ti plasmid and creation of a binary system

Barton et al. (1983) were the first researchers to demonstrate that the Ti plasmid could serve as a vector to carry foreign genes into plant cells. This finding led scientists to start addressing the potential use of this *Agrobacterium* behaviour as a tool to generate transgenic plants. Since then, scientists have developed a number of “binary-vector systems” to deliver foreign genes into plant genomes (Hoekema et al., 1983), including the destination vectors used in the Gateway® cloning protocol.

A binary-vector system has two components: a “disarmed” Ti plasmid (also called the *vir* helper plasmid), and a binary vector (Hoekema et al., 1983; de Framond et al., 1983). In the disarmed Ti plasmid, some of the natural features of the Ti plasmid are removed, including the T-DNA segments that are responsible for tumour formation and opine biosynthesis. At the same time, the characteristics of some of the transformation

machinery components that remain on the disarmed Ti plasmid are augmented. The second component of the binary-vector system is the binary vector itself. This vector is designed to contain unique restriction endonuclease sites for insertion of the modified T-DNA region together with the foreign DNA (Komori et al., 2007). These vectors allow propagation in both *Escherichia coli* and *Agrobacterium* cells, hence the referral to this vector/system as “binary”. A variety of selective markers, usually for antibiotic resistance, are also included in the binary vector backbone to allow easy selection of successfully transformed bacteria (Hellens and Mullineaux, 2000; Komori et al., 2007).

Further modifications of both the disarmed Ti plasmid and the binary vectors have made DNA manipulation and bacterial transformation easier and more efficient. Such modifications include the incorporation of more convenient multiple cloning sites and a reduction in the size of the vectors. When both of these vectors are present in the same *Agrobacterium* cell, products of the Ti plasmid act in *trans* on the modified T-DNA region of the binary vector to encourage DNA transport into plant cells (Hoekema et al., 1983). To further simplify the protocol, a number of *Agrobacterium* strains carrying the disarmed Ti plasmids have been created. As such, only one transformation (of the binary/destination vector) needs to be carried out when using these *Agrobacterium* strains (Hellens and Mullineaux, 2000).

1.3.7 *Agrobacterium*-mediated plant transformation

Since the discovery of the natural ability of *Agrobacterium* to integrate parts of its DNA into the plant genome, generation of transgenic plants without tissue culturing has become much more common, and as such, the attention has shifted to develop *Agrobacterium*-mediated *in planta* transformation protocols. Early protocols were initially developed using *Agrobacterium* 1) co-cultivated with plant seeds (Feldmann and Marks, 1987), 2) introduced into cut sites in plant apical shoot bases (Chang et al., 1994; Katavic et al., 1994), or 3) introduced into intact seedlings by means of vacuum infiltration (Bechtold and Pelletier, 1998). These approaches greatly reduced the “hands-on” time and expenses involved in tissue culture methodology.

Later in 1998, Clough and Bent simplified the method of Bechtold and Pelletier (1998) with a “floral dip” technique, in which *Arabidopsis* was transformed by dipping the

inflorescence into a culture of *Agrobacterium*, without the use of a vacuum or other pressurizing devices. Using this procedure, successful transformants can be selected readily with use of an antibiotic or herbicide resistance gene, followed by growth on media containing the selective agent.

The floral dip protocol has been modified and tailored to produce transgenics in plant species other than *Arabidopsis*, such as common wheat (*Triticum aestivum* L.) (Zale et al., 2009), Sorghum (*Sorghum bicolor* L. Moench) (El'konin et al., 2009), corn (*Zea mays*) (Chumakov et al., 2006), radish (*Raphanus sativus* L. *longipinnatus* Bailey) (Curtis and Nam, 2001), and oilseed (*Camelina sativa*) (Liu et al., 2012) crops.

1.4 Research objectives

The first objective of my study was to examine whether EB1b regulates root responses to mechanical stimulation through alterations of root elongation. I measured the lengths of roots exposed to two types of mechanical stimulation: 1) a transient mechanical stimulation generated by growing roots on an impenetrable surface placed at two different reclined angles, and 2) a constant mechanical impedance imposed by growing roots through agar media containing different concentrations of agar. Lengths of *eb1b-1* mutant, wild type, and EB1b overexpressor roots growing through air and agar of two different concentrations were compared.

The second objective of my study was to investigate how EB1b regulates root responses to transient mechanical stimulation. As described in section 1.2.3, EB1 has two functional domains: a protein-protein interacting domain at the C-terminus and a microtubule plus-end interacting domain at the N-terminus. To assess whether these two domains play a role in the process, transgenic *eb1b-1* mutant plants expressing either C- or N-terminal truncated versions of EB1b were generated. Root growth patterns of transgenic plants expressing a C-terminal tail truncation of EB1b were analyzed.

Chapter 2 Materials and Methods

2.1 Media

2.1.1 Bacterial growth

Escherichia coli cells were propagated at 37°C in Luria-Bertani (LB) broth (Bio101 Inc., Carlsbad, USA) with aeration, or on solid LB agar media (QBiogene, Carlsbad, USA). *Agrobacterium tumefaciens* cells were propagated at 30°C in yeast extract-mannitol (YM) broth (0.04% (w/v) yeast extract, 1% (w/v) mannitol, 0.01% (w/v) NaCl, 0.02% (w/v) $MgSO_4 \cdot 7H_2O$, and 0.05% (w/v) $K_2HPO_4 \cdot 3H_2O$ (Vincent, 1985), brought to a pH of 7.0 using 5M HCl) with aeration, or on solid YM media containing 1.5% agar. Kanamycin (Sigma-Aldrich, Oakville, Canada) was added at a final concentration of 50 µg/ml in the media when indicated.

2.1.2 Plant transformation

A. tumefaciens cultures were resuspended with infiltration media containing 5% (w/v) sucrose, and 0.02% (w/v) Silwet-7 (LEHLE SEEDS, Round Rock, USA) (Clough and Bent, 1998).

2.1.3 Plant growth

All *Arabidopsis* seeds were grown on 0.5X Murashige and Skoog (MS) (1962) basal salt mixture (Sigma-Aldrich), supplemented with 1% (w/v) sucrose, and 0.05% (w/v) 4-morpholineethanesulfonic acid (MES; Sigma-Aldrich), and brought to a pH of 5.8 using 5M KOH. Phytoblend agar (Caisson Laboratories, North Logan, USA) was added to the MS media as a solidifying agent, at the indicated concentrations. Hygromycin B (Sigma-Aldrich) was added at a final concentration of 30 µg/ml in the MS media when indicated.

2.2 Plant material

All of the *Arabidopsis* lines used were of the Wassilewskija (Ws) ecotype. Wild type seeds were obtained from the Arabidopsis Biological Resources Center (Columbus, USA). The EB1b mutant (*eb1b-1*) was generated previously by the insertion of T-DNA into the *EB1b* gene of *Arabidopsis* wild type plants and identified by screening the BASTA population at the Wisconsin Knockout Facility (Bisgrove et al., 2008). The EB1b overexpressing line (EB1b OX) was generated previously by the insertion of T-DNA carrying a full *EB1b* cDNA, under the transcriptional control of the *EB1b* promoter, into *Arabidopsis eb1b-1* mutant plants (Squires, 2013).

2.3 Plant growth conditions

All seeds collected were sterilized using the vapour phase method described by Clough and Bent (1998). Briefly, seeds were incubated in a sealed container filled with the vapour produced from a mixture of 3 ml of concentrated hydrochloric acid and 100ml of 7.5% sodium hypochlorite for a period of 1.75 hours. Seeds were then placed on an MS agar surface, and vernalized in the dark at 4°C for three days, after which the plates were transferred to the growth chamber (20°C, under a 16-hr-light/8-hr-dark cycle). The durations of the growth periods were as indicated.

2.4 Bacterial transformations

2.4.1 *Escherichia coli*

Vectors were introduced into One Shot® Top10 chemically-competent *E. coli* cells (Life Technologies Inc., Burlington, Canada) by heat shock transformation, as per the protocol provided by Life Technologies. Briefly, vectors were added to the *E. coli* culture, and the mixtures were allowed to chill on ice before placing them in a 42°C water bath. Super optimal broth with catabolite repression (S.O.C. broth) (Life Technologies Inc.) was then added to the heat-shocked cell/DNA mixture, and the culture was incubated at 37°C in a Forma Orbital shaker (Thermo Fisher Scientific Inc., Waltham, USA) with aeration for one hour. *E. coli* clones carrying vectors with *EB1b* inserts were selected by

plating on LB agar containing kanamycin. These vectors were subsequently extracted from the cells using a QIAprep® Spin Miniprep Kit (QIAGEN Inc., Toronto, Canada).

2.4.2 *Agrobacterium tumefaciens*

Vectors were introduced into ElectroMAX™ *A. tumefaciens* LBA4404 cells (Life Technologies Inc.) by electroporation, as per the protocol provided by Life Technologies. Briefly, a mixture of vectors and bacterial cells was added to the electroporation cuvette (Sigma-Aldrich), and electroporation was performed at 2.5 kV in an Eppendorf® Electroporator 2510 (Eppendorf AG, Mississauga, Canada). YM broth was subsequently added to the electroporated cells, and the culture was incubated at 30°C with aeration for three hours. *A. tumefaciens* clones carrying vectors containing *EB1b* inserts were selected by plating on YM agar media containing kanamycin.

2.5 PCR, electrophoresis, and DNA precipitation

This PCR protocol was used as the base for all of the PCR amplifications. The following ingredients were added to individual PCR tubes: 1 unit (U) Phusion® High-Fidelity DNA polymerase (New England BioLabs Ltd., Whitby, Canada), 1x Phusion® High-Fidelity buffer (New England BioLabs Ltd.), 200 µM dNTPs (Thermo Fisher Scientific Inc.), 3% DMSO (New England BioLabs Ltd.), DNA templates, 0.5 µM forward (F) primers, and 0.5 µM reverse (R) primers (Integrated DNA Technologies Inc., Toronto, Canada). Specific DNA template and primer pairs were added as indicated. PCR amplification was performed using a DNA Engine® thermal cycler (Bio-Rad Laboratories Inc., Mississauga, Canada). An initial denaturation cycle of three minutes at 98°C was performed; followed by 35 cycles of denaturation for 10 seconds at 98°C, annealing for 30 seconds at the specific temperature indicated, and extension for 90 seconds at 72°C; and one cycle of final extension for eight minutes at 72°C.

Amplified PCR products were size fractionated in a 1% agarose gel. Electrophoresis was carried out in 1x Tris-acetate-EDTA (TAE) buffer (40 mM Tris-acetate (pH 8.0), 1 mM EDTA) at 40 V. Gels were stained with Invitrogen™ SYBR® Safe DNA dye (Life Technologies Inc.), and photographed under UV illumination.

PCR products were excised from the agarose gels and purified using a QIAquick® gel extraction kit (QIAGEN), following the manufacturer's instructions. Using a modified protocol of Sambrook et al. (1998), purified PCR products were subsequently precipitated and resuspended in AccuGENE™ molecular grade water (Lonza Group Ltd., Mississauga, Canada). Briefly, the purified PCR product was mixed with 0.1 volumes of 2.5 M ammonium acetate and 2.5 volumes of ethanol, and chilled at -20°C overnight. The following day, the DNA was pelleted by centrifugation, and the supernatant was removed. After the DNA pellet was dried, AccuGENE™ molecular grade water was used to resuspend the DNA.

2.6 Restriction digests

All restriction endonuclease reactions were carried out at 37°C for 1.25 hours, followed by an incubation of 20 minutes at 80°C. For each reaction, 5 U of enzyme were added to 0.5 µg of DNA, with the buffer provided by the manufacturer. The hydrolyzed products were size fractioned by gel electrophoresis.

2.7 DNA sequencing

Plasmid DNA samples were sent to Eurofins MWG Operon LLC (Louisville, USA) for automated Sanger sequencing (Smith et al., 1986). Approximately 2 µM of each indicated primer was used in each of the dideoxy sequencing reactions (see Table 2.1). Primers F13 and R13 were provided by Eurofins MWG Operon LLC. Results of the DNA sequencing reactions were viewed using Chromas software (Technelysium Pty Ltd., South Brisbane, Australia).

Table 2.1 Primers used in PCR amplifications to produce EB1b truncations, in the modified Gateway® cloning protocol, and in DNA sequencing reactions

Primer name	Primer sequences (5' to 3') used in
	PCR amplifications to produce EB1b truncations
F1	GGGGACAAGTTTGTACAAAAAAGCAGGCTTCTTCTCCTCTTTTTCTTTGTTTTCG
F2	GTTCAAAAGGATCCATGGAGTTTCTTCAATGGTTGAAACGTT
R1	GGGGACCACTTTGTACAAGAAAGCTGGGTCCTAGAGATCAACCGAGACCTTGAG
R2	GGGGACCACTTTGTACAAGAAAGCTGGGTCGAGATCAACCGAGACCTTGAG
R3	GGGGACCACTTTGTACAAGAAAGCTGGGTCCTATGCGTATAATATCTTCTTAACCGCTAC
R4	GGGGACCACTTTGTACAAGAAAGCTGGGTCTGCGTATAATATCTTCTTAACCGCTAC
R5	GGGGACCACTTTGTACAAGAAAGCTGGGTCCTAAGTTTGGGTCTCTGCAGCAGC
R6	GGGGACCACTTTGTACAAGAAAGCTGGGTCAGTTTGGGTCTCTGCAGCAGC
R7	CAACCATTGAAGAAACTCCATGGATCCTTTTGAACCCC
	the modified Gateway® cloning protocol
F6	GTTTTCCCAGTCACGACGTT
R12	AACCTTTCTTCTCCGTCCT
	DNA sequencing reactions
F3	GCTTTCTTCCTCGACCAATG
F4	CCTACCTTACACATATCTTGTTGG
F5	GAAAAAAGAGGCTTCTTTCGTTTC
F13	TGTAAAACGACGGCCAGT
R8	GAACCCCTCTCTGAAACG
R9	GAGATGAGGGTATTAAAATTAGTTGTC
R10	CCTCCTTTGACAGAGCTTGC
R11	CCTCAAGCCCTAGAGACTGGT
R13	CAGGAAACAGCTATGACC

2.8 Creation of *EB1b* fragments with truncations

A total of six truncated *EB1b* constructs were created using PCR, four of which were constructs with C-terminal truncations in EB1b (EB1bΔC1 and EB1bΔC2 have 89 and 50 amino acid residues removed from the EB1b C-terminus, respectively; EB1b[ΔC1]-GFP and EB1b[ΔC2]-GFP are translational fusions of GFP to the C-terminus of EB1bΔC1 and EB1bΔC2), and the remaining two were constructs with N-terminal truncations in EB1b (EB1bΔN has 104 amino acid residues removed from the EB1b N-terminus, and EB1b[ΔN]-GFP is a translational fusion of GFP to the C-terminus of EB1bΔN). All constructs were created using a pCAMBIA 1300 DNA vector containing the *EB1b* promoter (1.5 kb upstream of the translational start codon) and the full length *EB1b* cDNA (courtesy of Dr. R. Dixit, Department of Biology, Washington University, St. Louis, USA).

To generate *EB1b* products with C-terminal truncations (i.e., for EB1bΔC1, EB1b[ΔC1]-GFP, EB1bΔC2, and EB1b[ΔC2]-GFP), PCR amplifications (as described in section 2.5) were carried out. The annealing temperatures for the amplification of EB1bΔC1 and EB1b[ΔC1]-GFP were 62°C, whereas the annealing temperatures for the amplification of EB1bΔC2 and EB1b[ΔC2]-GFP were 68°C. Primer pairs F1 and R1, F1 and R2, F1 and R3, and F1 and R4 were used to generate EB1bΔC1, EB1b[ΔC1]-GFP, EB1bΔC2, and EB1b[ΔC2]-GFP, respectively (Table 2.1).

To generate EB1bΔN, three-step (overlap extension) PCR amplification was carried out. Two PCR products were amplified from the pCAMBIA 1300 DNA vector in the first step: the *EB1b* promoter and the *EB1b* cDNA with an N-terminal truncation. To amplify both of these DNA molecules, PCR reactions were carried out (as described in section 2.5) using an annealing temperature of 60°C. Primer pairs of F1 and R5, and F2 and R6, were added to amplify the *EB1b* promoter and *EB1b* cDNA with an N-terminal truncation, respectively. In the second step of the three-step (overlap extension) PCR, the *EB1b* promoter and *EB1b* cDNA with an N-terminal truncation were ligated using the PCR protocol described in section 2.5, with the following modifications to the procedure: no initial denaturation was performed; 10 cycles of amplification were used (in place of 35 cycles); during the 10 cycle-reaction, the denaturation step was carried out for 30 seconds (in place of 10 seconds), the annealing step was performed at 65°C for 25

minutes (in place of 30 seconds), and the extension took place over 5 minutes (rather than 90 seconds); and there was no final extension. The ingredients for this PCR amplification were as described in section 2.5, except no primers were added. In this procedure, the two PCR products generated in the first step (the *EB1b* promoter and *EB1b* cDNA with an N-terminal truncation) served as both the DNA templates and the primers.

In the third step of the three-step (overlap extension) PCR, the ligated PCR products were further amplified by PCR. The annealing temperature for this reaction was 65°C, and the primers used were F1 and R6.

To generate the EB1b[ΔN]-GFP construct, the same procedure of three-step (overlap extension) PCR was carried out, with the following modification: in both the first and the third steps, primer R7 was used (in place of R6).

2.9 Modification of Gateway® cloning technology and bacterial transformation

A modified Gateway® cloning protocol was used to generate all of the clones carrying the truncated *EB1b* constructs. Insertion of final *EB1b* PCR products (created as described in section 2.8) into the donor vector pDONR™221 (Life Technologies Inc.) was carried out using the Gateway® BP Clonase® II Enzyme mix (Life Technologies Inc.), as per the manufacturer's instructions. The resulting recombinant products were subsequently introduced into *E. coli* cells by heat shock transformation, with selection of successful transformants as described in section 2.4.1. Entry vectors were subsequently extracted from the transformed cells using a QIAprep® Spin Miniprep Kit (QIAGEN), following the manufacturer's instructions. Restriction digests using *Bsp*HI (New England BioLabs Ltd.) were used to confirm that the selected entry vectors contained appropriate-sized (*EB1b*) inserts. DNA sequencing was used to determine the sequences of the inserts, using primers F4, F5, F13, R8, R9, and R13 (Table 2.1), and verify that these inserts were indeed *EB1b*.

EB1b inserts, along with the Gateway® *att*L attachment sites, were amplified from the entry vectors using PCR. In these PCR amplifications, entry vectors were used as the templates. Primers F6 and R12 were added. Changes in the PCR conditions were as follows: the initial denaturation was carried out for 20 seconds (in place of three minutes); during the 35-amplification cycles, the duration of the denaturation step was 20 seconds (in place of 10 seconds), the annealing step was carried out at 67°C for 20 seconds (in place of 30 seconds), and the extension step was performed for 75 seconds (in place of 90 seconds); 1 cycle of final extension was carried out for 5 minutes (in place of 8 minutes).To generate expression vectors carrying EB1bΔC1, EB1bΔC2, and EB1bΔN, the corresponding PCR products were recombined into the destination vector pMDC99 (Curtis and Grossniklaus, 2003) using the Gateway® LR Clonase® Enzyme mix (Life Technologies Inc.), as per the manufacturer's protocol. To generate expression vectors carrying EB1b[ΔC1]-GFP, EB1b[ΔC2]-GFP, and EB1b[ΔN]-GFP, the destination vector pMDC107 was substituted for pMDC99 (Curtis and Grossniklaus, 2003). These expression vectors were subsequently introduced into *E. coli* cells by heat shock transformation, and successful transformants were selected using the method described in section 2.4.1.

Double restriction digests using *Bsp*HI and *Ban*II (New England BioLabs Ltd.) were carried out to confirm that the selected expression clones carried proper-sized (*EB1b*) inserts. DNA sequencing was utilized to determine insert sequences, using primers F3, F4, F5, R8, R9, R10, and R11 (Table 2.1), and verify that these inserts were indeed *EB1b*. Verified expression vectors were introduced into *A. tumefaciens* cells by electroporation, and successful transformants were selected using the method described in section 2.4.2.

2.10 *Agrobacterium*-mediated plant transformation

Arabidopsis thaliana eb1b-1 mutant plants were used in the *Agrobacterium*-mediated plant transformation for all six *EB1b* truncations. The floral dip procedure of plant transformation carried out was based on the work of Clough and Bent (1998). Briefly, *eb1b-1* mutant plants were grown in the soil until just bolting. Bacterial cells were grown to an $OD_{600} \approx 2.00$, then pelleted and resuspended in infiltration media. Floral

buds were dipped in the *Agrobacterium*-filled infiltration media for at least 10 seconds. The dipped plants were placed on their sides in a tray covered with a transparent dome for approximately16 hours in the growth chamber. The dome was then removed and the plants were stood upright. After four days, these plants were dipped again using the same procedure. The floral-dipped plants were then allowed to self-fertilize.

2.11 Identification of homozygous transformed plants

Primary transformed (T_0) seeds produced from the floral-dipped plants were collected and selected for hygromycin B resistance (hyg^R) by growing them on an MS medium containing 0.8% phytoblend agar and hygromcyin B for five days. Hyg^R T_0 seedlings were transplanted into soil, and allowed to grow and self-fertilize. Populations of T_1 seeds from each transformed line were tested for a ratio of three hyg^R to one hygromycin sensitive (hyg^S) on an MS agar medium containing hygromycin B. A chi-square test was used to determine the fitness of this ratio. For each transformed line that showed a ratio of three hyg^R to one hyg^S, up to 40 T_1 seedlings were transferred into soil, where they were allowed to grow and self-fertilize. T_2 seeds produced from the T_1 plants of each transformed line were tested for 100% hyg^R on an MS agar medium containing hygromycin B. Further root analyses were carried out using the populations of T_2 seeds that were confirmed to be 100% hyg^R.

2.12 Root analyses

Arabidopsis seeds were placed on the agar surface of an MS medium containing 0.8%, 1.2% or 2.4% phytoblend agar and placed in the growth chamber. For the duration of the growth period, the agar plates were placed in the vertical position or reclined to an angle of 45˚ from vertical. The position of the root tip was marked on the back of the plates on the third day of incubation, and seedlings were grown for another 4 days. Images of roots were photographed using a Qimaging RetigaTM 4000R digital camera mounted on an Olympus® SZX16 stereo microscope. Photographic images were captured using QCapture Pro 6 software (QImaging, Surrey, Canada). Root skewing angles and lengths were measured on the photographs using ImageJ software (National

Institutes of Health, Bethesda, USA). The length or skewing angle of each root was measured from the mark denoting root tip position on the third day to the root tip position on the seventh day.

2.13 Statistical analysis

Pearson's chi-square tests were used to assess goodness of fit between the expected and observed Mendelian ratios of three hyg^R to one hyg^S seedlings. P-values were calculated using Microsoft Excel (Microsoft Canada Co., Mississauga, Canada). Population designations as hyg^R and hyg^S were assigned based on $P \geq 0.05$ and $P < 0.05$, respectively. For all root analyses, Student's t-tests were carried out using JMP®12 (SAS Institute Inc., Cary, USA).

Chapter 3 Results

3.1 Design of EB1b deletions

I am interested in determining whether the ability of EB1b to interact with other cellular components and/or track microtubule plus-ends plays a role in root responses to mechanical stimulation in *Arabidopsis*. The C-terminal protein-protein interaction domain or the N-terminal microtubule binding domain of EB1b was removed in the mutational analysis. A total of six constructs were designed: two that encode EB1b proteins with different sized deletions at the C-terminus, one that encodes the EB1b protein with a deletion at the N-terminus, and three that encode C-terminal GFP fusions to the three truncated proteins described above (Figure 3.1).

Two of the C-terminal EB1b deletion constructs were designed to remove the protein interaction ability of EB1b. In crystallography studies, Honnappa et al. (2005) and Slep et al. (2005) have shown that the EB homology domain of the human EB1 dimer is comprised of two α-helically coiled coils that mediate the dimerization of two EB1 monomers through the formation of a four-helix bundle. This four-helix bundle forms binding pockets for other +TIPs. Several mutational analyses have demonstrated that human EB1 with a deletion in the EB homology domain loses its ability to interact with non-tubulin components in the cell (Honnappa et al., 2005 and 2009; Bu and Su, 2003). Other studies have shown that the C-terminal acidic tail of human EB1 comprises a motif that also serves as binding sites for other cellular components (Weisbrich et al., 2007; Mishima et al., 2007; Dixit et al., 2009). Therefore I designed one *Arabidopsis* C-terminal deletion construct (EB1bΔC1) that consists of 204 of the usual 293 amino acid residues (i.e., with 89 residues removed from the C-terminus) of the full length EB1b protein. The EB1bΔC1 protein encodes a Calponin Homology (CH) domain (the microtubule-binding site at the N-terminus) and a linker region, but lacks the EB homology domain and tail region. I also designed another C-terminal deletion construct (EB1bΔC2) that consists of

243 of the usual 293 amino acid residues (i.e., with 50 residues removed from the C-terminus) of full length EB1b. This EB1bΔC2 deletion construct encodes an EB1b protein without the C-terminal tail region.

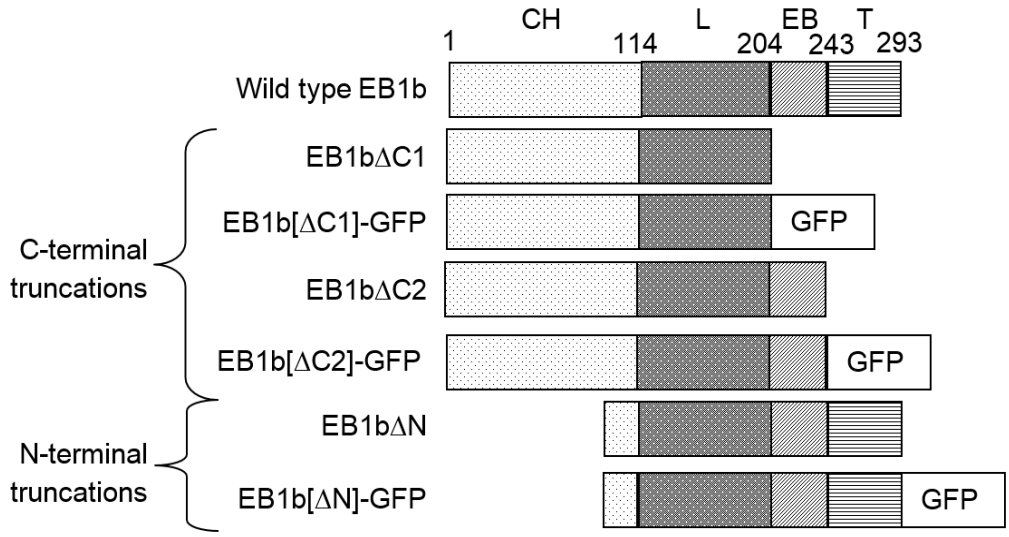

Figure 3.1 Schematic illustration of EB1b deletion constructs

EB1b constructs were designed, in which a portion of either the protein-protein interaction (C-terminal) or the microtubule plus-end binding (N-terminal) domain are removed. The wild type EB1b protein consists of a calponin homology domain (CH; amino acid residues 1-114), a variable linker region (L; amino acid residues 115-204), an EB homology domain (EB; amino acid residues 205-243), and a tail region (T; amino acid residues 244-293). The numbers above the diagram represent amino acid residue positions in *Arabidopsis* EB1b. The domains of EB1b in the figure is not drawn to scale. Four constructs have C-terminal truncations: EB1bΔC1, EB1b[ΔC1]-GFP, EB1bΔC2, and EB1b[ΔC2]-GFP. EB1bΔC1 has an 89 amino acid residue deletion from the C-terminus of EB1b which removes the EB homology domain and the tail region. In contrast, EB1bΔC2 has a smaller deletion (50 amino acid residues) at the C-terminus of EB1b. It removes the tail region of EB1b. Two constructs with N-terminal truncations were also made: EB1bΔN and EB1b[ΔN]-GFP. In the EB1bΔN construct, 104 amino acid residues from the N-terminus were removed. Constructs containing -GFP represent translational fusions of the green fluorescent protein to the C-terminus of each EB1b deletion.

EB1 family members are known for their ability to track microtubule plus-ends. In a crystallography study, Hayashi and Ikura (2003) demonstrated that the N-terminus of EB1 contains a CH domain. This domain allows EB1 to interact with microtubules. EB1 missing its CH domain has been shown to lose its ability to track microtubule plus-ends normally (Bu and Su, 2003; Skube et al., 2010; Komaki et al., 2010). To examine whether such microtubule plus-end tracking activity plays a role in root responses to mechanical stimulation, I designed an *Arabidopsis* N-terminal deletion construct (EB1bΔN). EB1bΔN encodes 189 amino acid residues with 104 residues removed from

the N-terminus of full length EB1b. EB1bΔN was designed to remove the ability of EB1b to bind microtubule plus-ends. This truncated version of EB1b consists of a linker, an EB homology domain, and a tail region, and is lacking the N-terminal CH domain.

The last three EB1b deletion constructs I created are GFP fusion versions of the three EB1b deletion constructs described above, and are designated as EB1b[ΔC1]-GFP, EB1b[ΔC2]-GFP, and EB1b[ΔN]-GFP. In a previous study, Squires (2013) found that in the roots of *eb1b-1* mutant plants over-expressing full length EB1b protein with GFP attached to the C-terminus (EB1b-GFP), the GFP-tagged protein localized correctly to the microtubule plus ends. These plants displayed similar responses to a combination of mechanical and gravitational stimulation as the *eb1b-1* mutant plants themselves, although transgenic mutants expressing full-length EB1b lacking a GFP tag responded in manner similar to wild type plants. These results suggest that the GFP moiety may be interfering with the function of the carboxy-terminus of EB1b. Therefore, the GFP fusion constructs that I generated were used to assess sub-cellular localization patterns of the EB1b truncated proteins, and were not used in root assays. Unfortunately, antibodies that specifically recognize EB1b and not EB1a or EB1c family members are unavailable and would be difficult to obtain given the high level of amino acid identity shared by these three *Arabidopsis* family members.

3.2 Production of *EB1b* cDNA fragments with C- or N-terminal truncations

EB1b deletion constructs were made using PCR amplifications from a full length EB1b cDNA template that included the native 5' promoter sequences of EB1b from *Arabidopsis* (Figure 3.2). Sequences of Gateway®-compatible *att*B attachment sites were added to the 5' end of each primer and were subsequently added onto both 5' and 3' ends of the final truncated *EB1b* cDNA products.

PCR products were separated on agarose gels by electrophoresis. The expected sizes of the PCR products for EB1bΔC1, EB1b[ΔC1]-GFP, EB1bΔC2, and EB1b[ΔC2]-GFP were 2,191 bp, 2,188 bp, 2,308 bp, and 2,305 bp, respectively. (The GFP portion had not been added to these constructs yet; the three base pair difference in size was

due to the removal of a stop codon at the end of both EB1bΔC1 and EB1bΔC2 prior to the attachment of the GFP). No apparent differences were observed between the expected band sizes and the actual band sizes on the agarose gels (Figure 3.3A and 3.3B). PCR products matching the expected sizes were extracted from the gels and used in recombination reactions with Gateway® vectors.

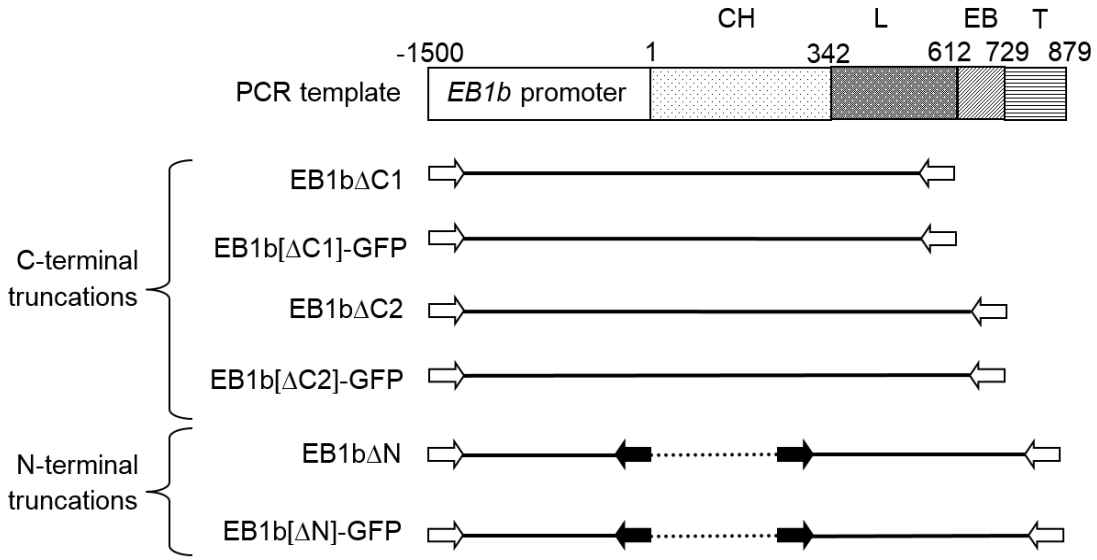

Figure 3.2 Schematic illustration of primer designs for generation of EB1b truncations

Full EB1b cDNA and upstream EB1b promoter sequences were used as a template in PCR reactions to generate EB1b truncations. The numbers above the template represent nucleotide positions. Sections of the EB1b PCR template are not drawn to scale. All arrows represent primers and are placed in the positions where they anneal to the template. Solid lines represent the nucleotide sequences being amplified. The resulting PCR products are as follows: EB1bΔC1 (consists of the EB1b promoter followed by the 1st - 612th bp), EB1bΔC2 (consists of the EB1b promoter followed by the 1st - 729th bp), and EB1bΔN (consists of the EB1b promoter followed by the 313th - 879th bp). Sequences of Gateway®-compatible attachment (*att*B) sites were also added to the primer sequences depicted by open arrows. Primers were designed such that EB1bΔC1, EB1bΔC2, and EB1bΔN contain a stop codon at the 3' end. Three additional EB1b truncated PCR products were also generated in this manner, lacking the 3' stop codons, to be used in making GFP fusions of the three EB1b deletion products (i.e., EB1b[ΔC1]-GFP, EB1b[ΔC2]-GFP, and EB1b[ΔN]-GFP).

To generate EB1bΔN and EB1b[ΔN]-GFP cDNA fragments, three-step (overlap extension) PCR was used. Two PCR products were amplified in the first step: the *EB1b* promoter, and the *EB1b* cDNA containing an N-terminal truncation. The expected size of PCR products for the *EB1b* promoter was 1,564 bp for both the EB1bΔN and EB1b[ΔN]-GFP constructs (Figure 3.3C). The expected sizes of PCR products for the *EB1b* cDNA

with an N-terminal truncation were 615 bp and 612 bp for EB1bΔN and EB1b[ΔN]-GFP, respectively (Figure 3.3D and 3.3F). During the second step of the overlap extension PCR, the PCR products were used as both DNA templates and primers to produce chimeric PCR products. In this step, the *EB1b* promoter was connected to the 5' end of the *EB1b* cDNA with an N-terminal truncation. The final chimeric PCR products were further amplified in the third step of the overlap extension PCR. The expected chimeric PCR product sizes were 2,149 bp and 2,146 bp for EB1bΔN and EB1b[ΔN]-GFP, respectively. No apparent differences were observed between the expected band sizes and the actual band sizes on the agarose gels (Figure 3.3E and 3.3G). Chimeric PCR products were extracted from the gels and used in the modified Gateway® cloning procedure to generate expression vectors.

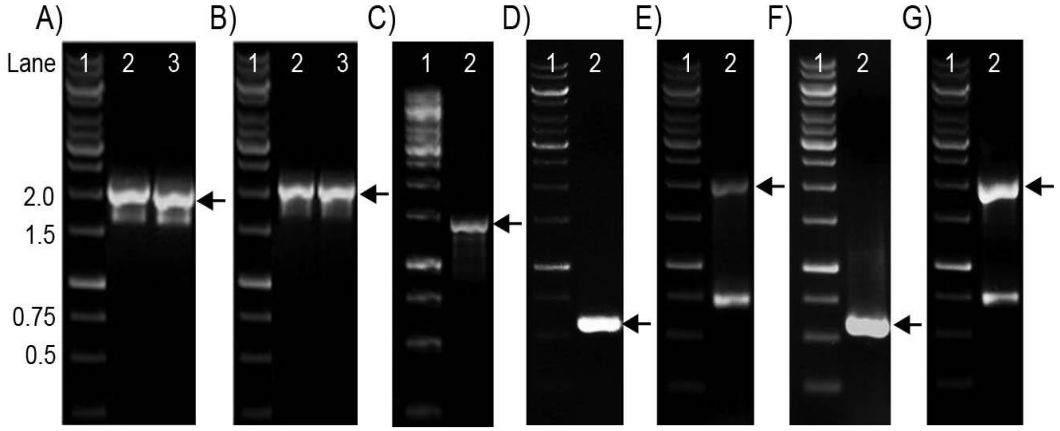

Figure 3.3 Production of *EB1b* cDNA fragments with N- or C-terminal truncations

Presented above are photographs of agarose gels containing PCR products used to generate constructs encoding truncated EB1b proteins. Lanes 2 and 3 of the agarose gel in (A) show PCR products used to generate EB1bΔC1 and EB1b[ΔC1]-GFP constructs, respectively. Lanes 2 and 3 in (B) show PCR products used to generate EB1bΔC2 and EB1b[ΔC2]-GFP constructs, respectively. The agarose gels in (C) to (G) show the PCR products amplified from a three-step (overlap extension) PCR used to generate N-terminal deletion constructs. Lane 2 in gel (C) shows the PCR product obtained from EB1b promoter sequences. Gels (D) and (F) show the EB1b cDNA with N-terminal truncations used to generate EB1bΔN and EB1b[ΔN]-GFP constructs, respectively. Gels (E) and (G) show chimeric PCR products containing the EB1b promoter and EB1b cDNA with N-terminal truncations for EB1bΔN and EB1b[ΔN]-GFP constructs, respectively. The first lane in all of the gels contains a DNA reference ladder. The arrows beside each gel indicate the position of the expected PCR products. Numbers beside (A) indicate the size of relevant bands (in kilobases) of the reference ladder.

3.3 Creation of expression vectors carrying truncated *EB1b* inserts using a modified Gateway® cloning system

In the traditional Gateway® cloning system, inserts are integrated into a donor vector by homologous recombination to generate an entry vector. The inserts are then transferred from the entry vector into a destination vector by homologous recombination to generate an expression vector. One of the main strategies to select the clones containing expression vectors on an agar medium is to utilize a destination vector that carries a different antibiotic resistant gene than the entry vector. However, both the entry and destination vectors that I had available to me carried the same antibiotic resistance gene, encoding kanamycin resistance. This means that I could not use antibiotic resistance to distinguish between bacterial clones containing expression vectors and those carrying entry vectors. To circumvent this problem, rather than ordering new vectors containing different selectable markers, I developed a modified version of the Gateway® cloning protocol (Figure 3.4). In the modified protocol, after homologous recombination takes place between the *att*B and *att*P sites (Figure 3.4A), the insert and flanking *att*L homologous recombination sites were amplified from the entry vectors by PCR (Figure 3.4B). After extraction from the gel, PCR products were integrated into destination vectors through homologous recombination (Figure 3.4C). Destination vectors that have not undergone homologous recombination with the PCR product will retain the suicide gene, and thus will not be selected for post-transformation. As a result of utilizing this modified protocol, bacterial cells successfully transformed with expression vectors carrying the desired inserts could be selected easily on the media.

Using the modified Gateway® cloning protocol, PCR products were recombined into donor vectors. The resulting recombinant entry vectors were transformed into *E. coli* cells, and up to eight bacterial clones containing entry vectors with *EB1b* inserts (i.e., without the presence of the suicide gene) were selected by plating on LB agar containing kanamycin. Bacterial clones carrying the desired entry vectors with *EB1b* inserts were verified by comparing DNA fragment sizes after restriction enzyme hydrolysis using *Bsp*HI. The expected sizes of the digestion products for the six constructs are as follows: A) 3,750 bp and 927 bp for EB1bΔC1, B) 3,747 bp and 927 bp for EB1b[ΔC1]-GFP, C) 3,867 bp and 927 bp for EB1bΔC2, D) 3,864 bp and 927 bp for EB1b[ΔC2]-GFP, E)

3,705 bp and 927 bp for EB1bΔN, and F) 3,702 bp and 927 bp for EB1b[ΔN]-GFP. No apparent differences were observed between the expected band sizes and the actual band sizes on the agarose gels (Figure 3.5). Entry vectors containing appropriate-sized inserts extracted from two bacterial clones were sent for DNA sequencing; six sequencing reads were performed for each vector sample. No errors were found in the nucleotide sequences of the *EB1b* inserts (data not shown). One entry clone was carried forward to generate PCR products containing *EB1b* inserts with Gateway®-compatible attachment (*att*L) sites.

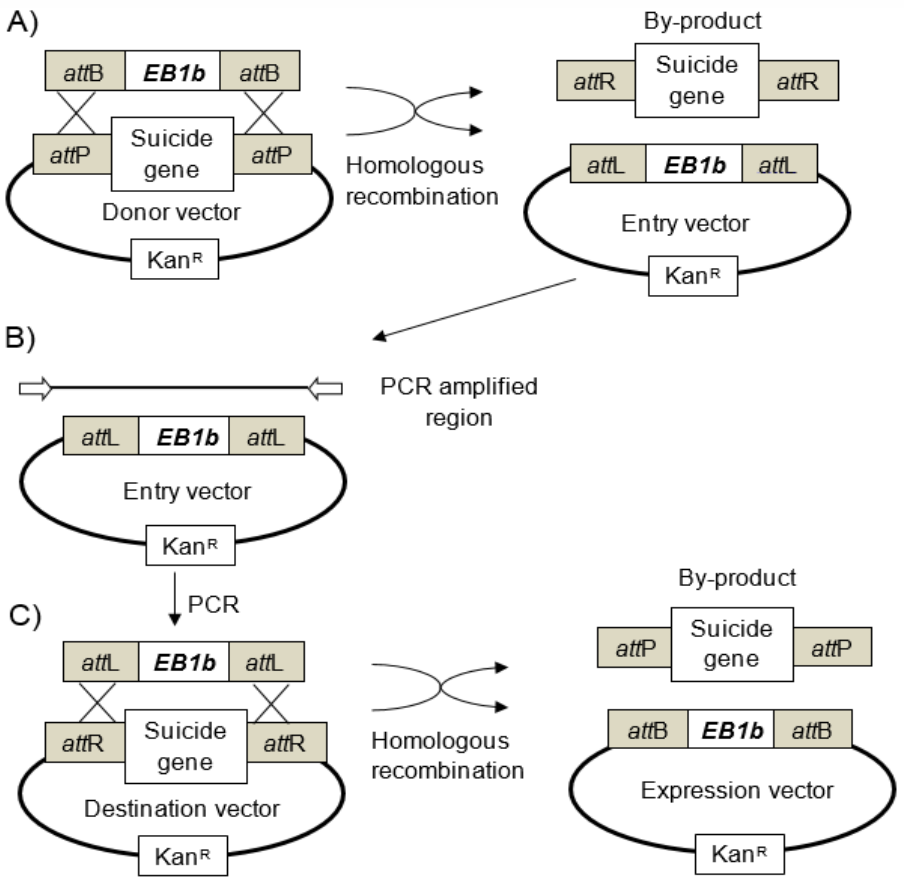

Figure 3.4 Schematic illustration of modified Gateway® cloning protocol

(A) Homologous recombination takes place between the *att*B sites of the *EB1b* fragments and the *att*P sites of the donor vectors. After transformation, selection of clones containing these vectors was carried out using kanamycin. The resulting entry vectors carry *EB1b* inserts and lack the suicide gene. (B) The *EB1b* insert, along with the *att*L sites, were amplified from the entry vectors by PCR. The arrows represent primers and their position marks the sites where they anneal to the vector. The solid line between the arrows represents the PCR product thus amplified from the entry vector. (C) This PCR product was subsequently recombined into destination vectors to generate expression vectors containing the *att*B-flanked *EB1b* truncated fragment.

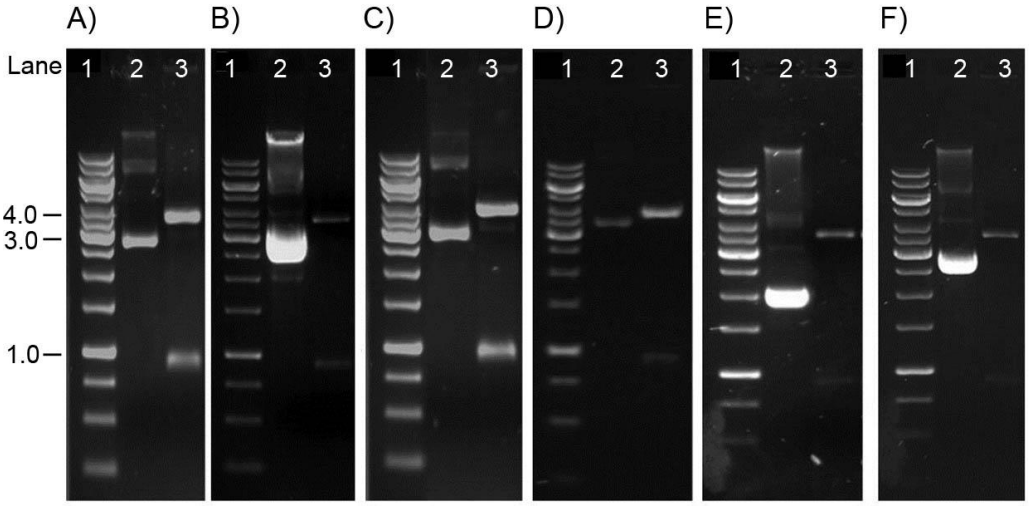

Figure 3.5 Restriction digests of entry vectors containing *EB1b* inserts

Products produced from entry vectors containing (A) EB1bΔC1, (B) EB1b[ΔC1]-GFP, (C) EB1bΔC2, (D) EB1b[ΔC2]-GFP, (E) EB1bΔN, and (F) EB1b[ΔN]-GFP constructs after digestion by the restriction endonuclease *Bsp*HI. Each photograph of the gel contains a DNA reference ladder in lane 1, an undigested vector sample in lane 2, and the vector hydrolysed with *Bsp*HI in lane 3. Numbers beside gel (A) indicate the size of relevant bands (in kilobases) of the reference ladder.

To amplify DNA fragments containing *EB1b* inserts along with Gateway™-compatible *att*L sites, EB1-containing entry vectors were used as templates in PCR reactions. The resulting PCR products were size-separated using agarose gel electrophoresis. The expected sizes of the PCR products for the six constructs are as follows: A) 2,449 bp for EB1bΔC1, B) 2,446 bp for EB1b[ΔC1]-GFP, C) 2,566 bp for EB1bΔC2, D) 2,563 bp for EB1b[ΔC2]-GFP, E) 2,404 bp for EB1bΔN, and F) 2,401 bp for EB1b[ΔN]-GFP. No apparent differences were observed between the expected band sizes and the actual band sizes on the agarose gels (Figure 3.6). Bands corresponding to the desired PCR products were excised from the gels. The DNA contained in these bands was extracted and used in the homologous recombination step between *att*L and *att*R in the modified Gateway® cloning procedure (Figure 3.4C).

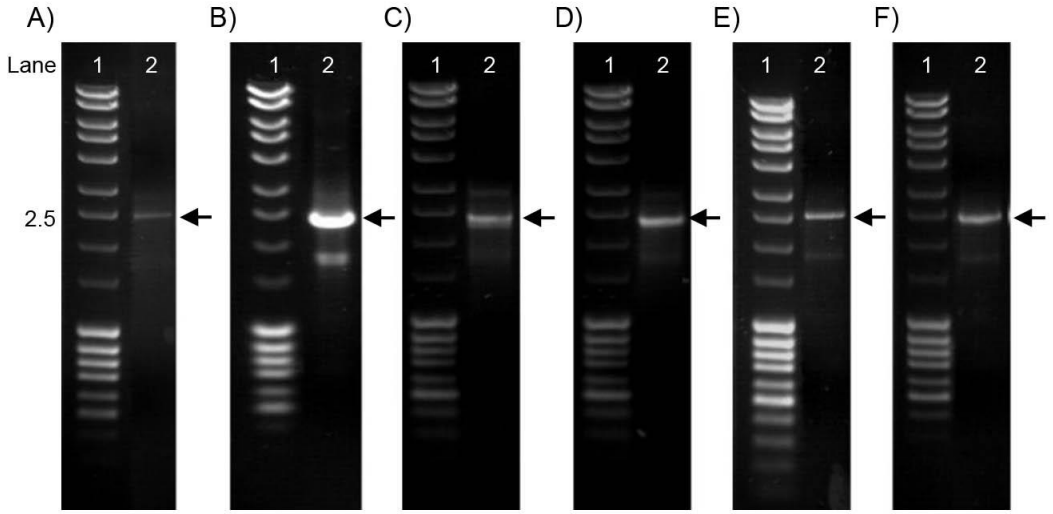

Figure 3.6 Truncated *EB1b* PCR products with Gateway™-compatible attachment (*att*L) sites

Truncated *EB1b* fragments with Gateway™-compatible *att*L sites were PCR-amplified from entry vectors carrying the *EB1b* insert. Each photograph of the gel shows a DNA reference ladder (lane 1) and PCR products (lane 2) corresponding to the EB1bΔC1 (A), EB1b[ΔC1]-GFP (B), EB1bΔC2 (C), EB1bΔ[[C2]-GFP (D), EB1bΔN (E), and EB1b[ΔN]-GFP(F) constructs. Arrows indicate bands that correspond to the expected PCR fragment sizes. The number beside gel (A) indicates the size of relevant bands (in kilobases) in the lane containing the reference ladder.

To generate expression vectors carrying *EB1b* inserts, PCR products containing truncated versions of the *EB1b* gene flanked by *att*L attachment sites were used in recombination reactions with the destination vector (Figure 3.4C). Recombinant products were subsequently transformed into *E. coli* cells. Up to eight bacterial clones were selected by plating on LB agar containing kanamycin. Bacterial clones carrying desired expression vectors with *EB1b* inserts were selected by comparing DNA fragment sizes after a double restriction digest using *Bsp*HI and *Ban*II. The resulting DNA fragments were size-separated by agarose gel electrophoresis. The expected digest product sizes for the vector containing the EB1b[ΔC1]-GFP construct were 5,873 bp, 3,371 bp, 1,916 bp, 757 bp, and 293 bp, while the expected digest product sizes for the vector containing the EB1b[ΔC2]-GFP construct were 5,873 bp, 3,371 bp, 2,033 bp, 757 bp, and 293 bp. EB1b[ΔC1]-GFP and EB1b[ΔC2]-GFP were the first two constructs to be tested with the double digest. No apparent differences were observed between the expected and actual band sizes on the agarose gels, except that the 293 bp band could not be seen (Figure 3.7), most likely because it was too faint to be detected, given its small size relative to the other bands on the gel. Nonetheless, this missing band meant that the double digest

test could not be used to verify that the expression vectors carried the proper EB1b inserts. Verification was accomplished by sending one expression vector from each *EB1b* truncation type (a total of six) for DNA sequencing; six sequencing reads were performed on each vector. No errors were found in the nucleotide sequences of the *EB1b* inserts (data not shown). One expression clone from each EB1b truncation type was transformed into *Agrobacterium* cells and bacterial clones were selected on the basis of their resistance to kanamycin.

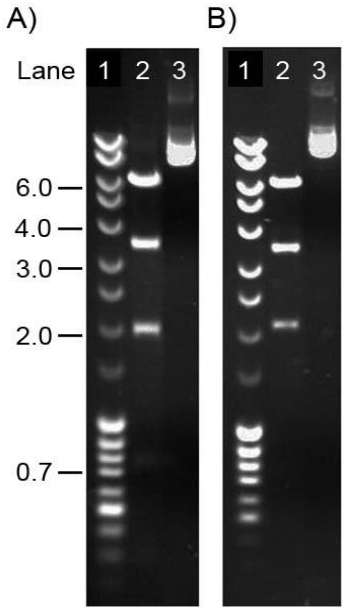

Figure 3.7 Restriction digests of expression vectors containing two of the *EB1b* truncations

Double restriction digest products produced from expression vectors containing EB1b[ΔC1]-GFP (A) and EB1b[ΔC2]-GFP (B), after hydrolysis by *Bsp*HI and *Ban*II. Each photograph of the gels contains a DNA reference ladder (lane 1), the vector digested with *Bsp*HI and *Ban*II (lane 2), and an undigested vector sample (lane 3). Numbers beside gel (A) indicate the size of relevant bands (in kilobases) in the lane containing the reference ladder.

3.4 Production of homozygous transgenic plants expressing EB1b deletion constructs

To create transgenic plants carrying EB1b deletion constructs, flowers of *eb1b-1* mutant plants were dipped in solutions containing *Agrobacterium* cells. This procedure allows the *Agrobacterium* to transfer EB1b inserts, along with the hygromycin resistant gene, randomly into the genome of plant cells. Dipped plants were allowed to self-

fertilize to produce primary transformants (T_0 seeds). Successful transformants were selected based on their resistance to hygromycin, an indication of the presence of an EB1b deletion construct. Hygromycin resistance is a dominant trait, and therefore one copy of the transgene is sufficient to provide the plant with antibiotic resistance. In the T_0 generation, seedlings are hemizygous with insertions at single or multiple loci. A range of 4-43 independent lines of hygromycin-resistant T_0 seedlings were identified for plants transformed with EB1b constructs (Table 3.1).

Table 3.1 Isolation of transgenic lines homozygous for single or multiple closely linked transgenes

	Generations		
	T_0	T_1	T_2
Constructs	Number of hyg^R seedlings isolated	Number of lines segregating 3 hyg^R : 1 hyg^S (number of lines tested)*	Number of lines producing 100% hyg^R (number of lines tested)
EB1bΔC1	43	4 (11)	3 (3)
EB1b[ΔC1]-GFP	4	3 (3)	in progress**
EB1bΔC2	11	7 (8)	5 (7)
EB1b[ΔC2]-GFP	17	3 (3)	in progress**
EB1bΔN	8	4 (5)	1 (1)
EB1b[ΔN]-GFP	6	3 (4)	in progress**

*A segregation ratio of 3 hyg^R : 1 hyg^S was determined by Pearson's chi-square test at $p>0.05$. **Genetic screening of transgenic plants has been passed on to Hae Ryoung Kim, the student who will continue with this project. hyg^R = hygromycin resistant. hyg^S = hygromycin sensitive.

Next, I looked for independent T_0 lines carrying either one or closely linked copies of the transgene. Given that the expression level of EB1b has been shown to affect root responses to mechanical cues (Squires, 2013), and that gene insertions at multiple unlinked loci would segregate as independent entities during meiosis (giving rise to progeny with differing numbers of transgenes and thus different transgene expression levels), finding such T_0 lines is essential if the phenotype is to be passed on to future generations faithfully in a true-breeding manner. To find these lines, I screened T_1 generation plants for a Mendelian ratio of three displaying hygromycin resistance (hyg^R) to one displaying hygromycin sensitivity (hyg^S). For each of the six EB1b deletion

constructs, between three and eleven independent T_1 lines were screened and between three and seven independent T_1 lines that fit this 3 hyg^R : 1 hyg^S ratio were found. These lines were then carried forward to the next step of genetic screening, where I looked for independent lines homozygous for the transgene. This was done by screening for 100% hygromycin resistance among T_2 lines produced from the T_1 seedlings previously screened for a Mendelian ratio of 3 hyg^R : 1 hyg^S.

For the EB1bΔC1 construct, a total of 43 hygromycin resistant seedlings (T_0) were grown from seeds produced by the *Agrobacterium*-dipped plants. These seedlings were grown to maturity and allowed to self-pollinate to form T_1 seeds. Seeds from 11 of these plants (T_1) were assayed for their resistance to hygromycin. Four of the 11 plants produced seeds showing a 3 hyg^R : 1 hyg^S ratio. T_2 plants were grown from these seeds. Seeds from three of these plants (T_2) were tested for hygromycin resistance. All three seed samples showed 100% hygromycin resistance.

For the EB1bΔC2 construct, 11 hygromycin resistant seedlings (T_0) were grown from seeds produced by the *Agrobacterium*-treated plants. These seedlings were grown to maturity and allowed to self-fertilize. Seeds from eight of these plants (T_1) were tested for their resistance to hygromycin. Seven of the eight plants produced seeds showing a 3 hyg^R : 1 hyg^S ratio. Seeds from all seven of these plants (T_2) were assayed for hygromycin resistance. Five of the seed samples displayed 100% hygromycin resistance.

For the EB1bΔN construct, a total of eight hygromycin resistant seedlings (T_0) were grown from seeds produced by the *Agrobacterium*-dipped plants. These seedlings were grown to maturity and allowed to self-pollinate. Seeds from five of these plants (T_1) were assayed for their resistance to hygromycin. Four of the five plants produced seeds showing a 3 hyg^R : 1 hyg^S ratio. Seeds from one of these plants (T_2) were tested for hygromycin resistance. This seed sample showed 100% hygromycin resistance.

Raw data for these genetic screens can be found in Appendix A, along with p-values for the Chi-square statistical tests carried out. Further screening for plants carrying EB1b[ΔC1]-GFP, EB1b[ΔC2]-GFP, EB1bΔN, and EB1b[ΔN]-GFP constructs has been passed on to the student who has taken over this project.

Table 3.2 provides a summary of the *Arabidopsis* lines used in the experiments that I carried out for this thesis, as well as those discussed within the thesis text.

Table 3.2 *Arabidopsis* lines used in experiments carried out for and discussed in this thesis

Line	Description	Reference
wild type	Wassilewskija (Ws) ecotype	Arabidopsis Biological Resources Center (Columbus, USA).
eb1b-1	T-DNA insertional mutant of Ws	Bisgrove et al., 2008
EB1b WX	Wild type expressed EB1b in *eb1b-1* mutant	Squires, 2013
EB1b-GFP	GFP fusion to the C-terminus of full length EB1b in *eb1b-1* mutant	Squires, 2013
EB1b OX	Overexpressed EB1b in *eb1b-1* mutant	Squires, 2013
EB1bΔC1	EB1b with 89 amino acid residues deleted at the C-terminus in *eb1b-1* mutant	this thesis
EB1b[ΔC1]-GFP	GFP fusion to the C-terminus of EB1bΔC1 in *eb1b-1* mutant	this thesis
EB1bΔC2	EB1b with 50 amino acid residues deleted at the C-terminus in *eb1b-1* mutant	this thesis
EB1b[ΔC2]-GFP	GFP fusion to the C-terminus of EB1bΔC2 in *eb1b-1* mutant	this thesis
EB1bΔN	EB1b with 104 amino acid residues deleted at the N-terminus in *eb1b-1* mutant	this thesis
EB1b[ΔN]-GFP	GFP fusion to the C-terminus of EB1bΔN in *eb1b-1* mutant	this thesis

3.5 Responses of roots expressing an EB1b C-terminal truncation to gravitational/transient mechanical stimulation

To determine whether the C-terminal tail domain of EB1b plays a role in root responses to transient mechanical stimulation, *eb1b-1* mutants transformed with the EB1bΔC2 construct were analyzed and compared with both *eb1b-1* (negative control) and wild type seedlings (positive control). Previous analyses have shown that mutant plants expressing full length EB1b at levels equivalent to wild type (EB1b WX) also have similar responses to touch/gravity as wild type (Squires, 2013). Root responses to a combination of gravitational and transient mechanical stimulation were assayed by growing seedlings at the back of agar plates reclined from a vertical orientation by an

angle of 45° (Figure 3.8A). Under these conditions, roots grow on the plastic surface of the Petri plate, which represents an impenetrable object. When the root tips touch the plastic surface of the plate, they are pushed against the Petri plate as the cells in the root elongation zone continue to expand. Since the roots cannot penetrate through the Petri plate, they buckle as a result of the force generated from cell expansion. The buckling displaces roots from a normal downward growing trajectory, and thus triggers gravitropic responses. Differential cell elongation rates across roots result in the formation of second bends that reorient the root tips back into parallel alignment with the gravity vector. As cell elongation continues, the root tips grow downward until they once again encounter the Petri plate, causing the regime to repeat. These repeating responses to the combination of gravitational and transient mechanical stimulation cause the roots to skew off to one side as they grow. As such, the skewing angle of the roots provides a measure of the plant response to the transient stimuli (provided here by the combination of touch and gravity sensing). Hence, I measured root skewing angles as an indication of the plant response to such stimulation in this assay.

I found that roots of all genotypes skewed towards the left when viewed from above the agar surface (Figure 3.8). As previously demonstrated in our laboratory, *eb1b-1* mutant roots had a skewing angle that was significantly greater than wild type (39.3° versus 19.4°; Student's t-test, $p<0.03$). Roots of the three EB1bΔC2 lines had average skewing angles of 46.6° for line 1 (L1), 44.9° for line 2 (L2), and 43.7° for line 3 (L3). There was no significant difference in root skewing angles between the three EB1bΔC2 lines (Student's t-test, $p>0.71$). Skewing angles in these transgenic lines were also equivalent to *eb1b-1* mutants (Student's t-test, $p>0.36$) and were significantly greater than wild type (Student's t-test, $p<0.009$). Recent reverse transcription followed by PCR analyses carried out in our laboratory indicate that the truncated version of EB1b is expressed in all three of these EB1bΔC2 mutant lines (Hae Ryoung Kim, personal communication). Thus, these results suggest that EB1b acts as an inhibitor of root responses to the combination of gravitational and transient mechanical stimulation, and the C-terminal EB1b tail domain appears to play a critical role in these responses.

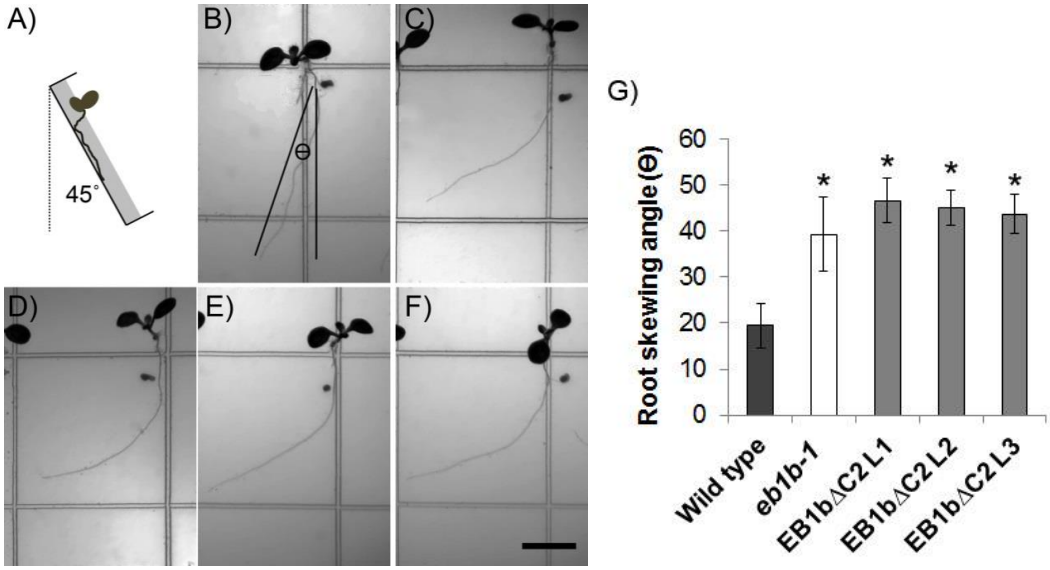

Figure 3.8 Effects of EB1b C-terminal tail deletion on root responses to mechanical/gravitational stimulation

Representative seedlings from seven-day-old wild type (B), *eb1b-1* mutant (C), and three transgenic lines (L1, L2, and L3) expressing EB1bΔC2 are shown (D, E, and F). Roots were grown under the agar along the back of plates placed at a reclined angle of 45° (see cartoon in (A)). The black mark beside each root indicates the root tip position on the third day of growth. Root skewing angle (Θ) was measured from the black mark to the root tip on the seventh day, as illustrated in (B). The size bar in (F) represents 5 mm and applies to all photographs. Each bar in (G) represents average root skewing angles of three biological replications with standard errors. A range of 13 to 41 roots were measured per genotype in each replicate for a total 79 to 118 roots per genotype. The asterisks denote a significant difference from the wild type (Student's t-test, $p<0.05$).

3.6 Root elongation rate in response to mechanical/gravitational stimulation

Next, I investigated whether EB1b regulates root responses to mechanical stimulation via the alteration of elongation rate of the root. In this experiment, I assessed the skewing angle and lengths of roots exposed to two different types of mechanical stimulation: 1) transient mechanical stimulation (provided by growing roots on the surface of agar plates reclined from a vertical orientation), and 2) constant mechanical impedance (imposed by growing roots through agar media).

In the first assay, roots were given transient mechanical stimulation by growing them on the agar surface of plates that were reclined from a vertical orientation. Two different levels of transient mechanical stimulation were generated by reclining the plates

by angles of 20° and 45°. How transient mechanical stimulation is generated in this assay, and how roots respond to this stimulation, is similar to the assay described above in section 3.5. The differences for this assay are that the agar surface represents the impenetrable object and roots are growing through the air, which imposes little to no constant mechanical impedance.

As shown in the photographs of Figure 3.9 (experiments published in Squires (2013), roots of all genotypes skew towards the left when viewed from above the agar surface, indicating that roots are responding to the combination of gravitational and transient mechanical stimulation. The *eb1b-1* mutant roots skew more than wild type when grown at either reclined angles of 20° or 45° (Squires, 2013). Thus, the *eb1b-1* mutant appears to be more sensitive to the cues encountered in this experiment. On the other hand, EB1b OX roots skew less than wild type, showing a lesser response to the stimulation. Therefore, comparing the skewing angles of the roots displayed by these three plant genotypes, it would appear that EB1b causes roots to display less sensitivity to gravitational/transient mechanical cues. This result was expected as it is in agreement with previous studies carried out by our lab (Squires, 2013; Bisgrove et al., 2008; Gleeson et al., 2012), as well as the observation reported in section 3.5 of this thesis.

Despite the difference in skewing angles, there was no significant difference in the root lengths I measured between the *eb1b-1* mutant and wild type genotypes when grown at either reclined angle (Student's t-test, $p>0.65$). The loss of EB1b had no significant effect on overall root elongation when roots were exposed to gravitational and transient mechanical stimulation. In fact, neither the *eb1b-1* mutant (Student's t-test, $p>0.39$) nor the wild type roots (Student's t-test, $p>0.89$) showed any significant difference in elongation rate between the two levels of transient mechanical stimulation provided. Thus, it would appear that roots do not change their elongation rate in response to the combination of gravitational and transiently applied mechanical stimuli. The overall rate of root elongation appears to be uncoupled from the response to such stimulation. The two responses seem to be controlled by different mechanisms within the root. The length of EB1b OX roots were shorter than the other two genotypes (Student's t-test, $p<0.0012$), and showed no significant difference in length when grown at either reclined angle (Student's t-test, $p>0.95$). Thus, it appears that EB1b has an inhibitory effect on root elongation, but only when overexpressed.

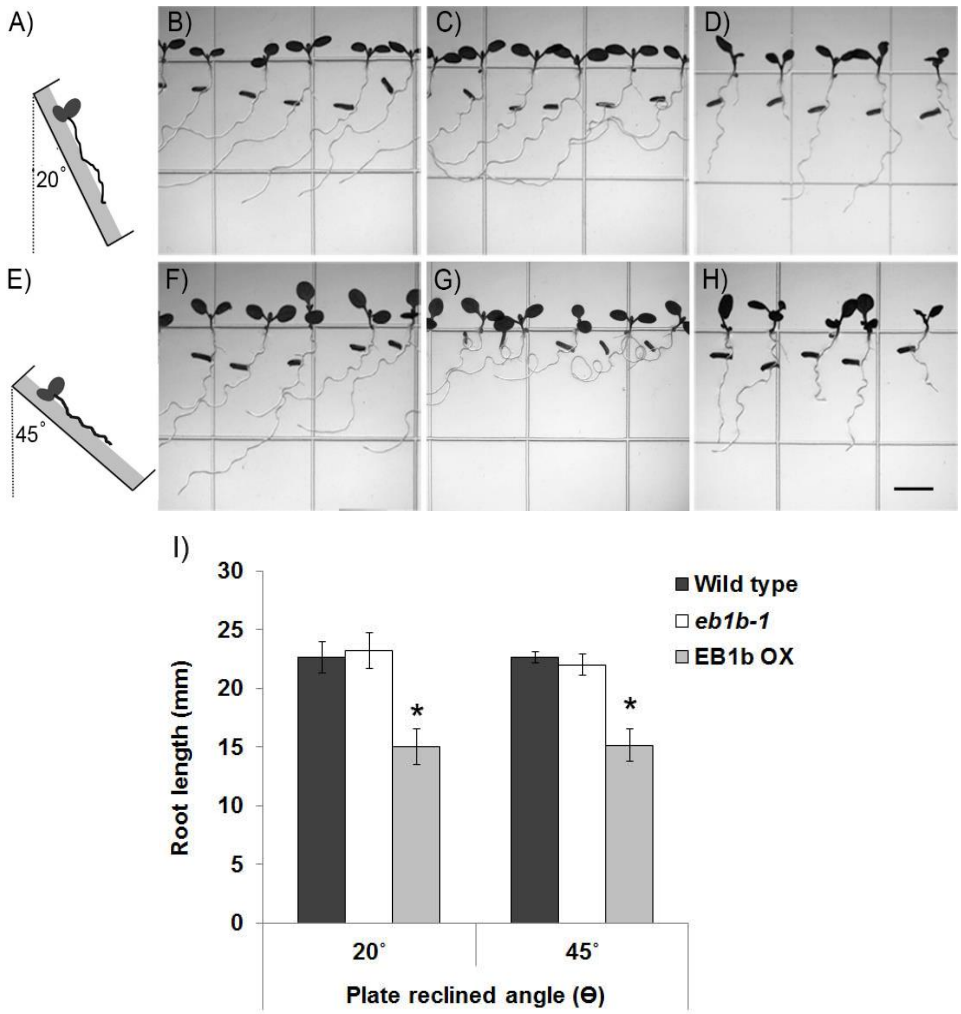

Figure 3.9 The level of transient stimulation does not affect overall rates of root elongation

Wild type (B, F), *eb1b-1* mutant (C, G), and EB1b OX (D, H) seedlings were grown on the surface of agar plates for seven days. Plates were placed at a reclined angle of 20˚ (top row of photographs) or 45˚ (bottom row of photographs), as schematically illustrated in (A) and (E), respectively. The black mark beside each root indicates the root tip position on the third day of growth. Root lengths were determined by measuring the distance along the root from the black marks to the root tips. The size bar in (H) represents 5 mm and applies to all photographs. Each bar in graph (I) represents average root lengths from six biological replicates with standard errors. A range of 12 to 40 roots per genotype on each plate angle were measured in each replicate, for a total of 101 to 180 roots per genotype for each plate angle. The asterisks denote significant differences in root length between the EB1b OX and either the wild type or *eb1b-1* mutant genotypes (Student's t-test, $p<0.02$), which did not differ significantly from each other (Student's t-test, $p>0.50$), grown at either reclined plate angle. (Photos for this figure were provided by S. Squires.)

In the second assay, roots were given constant mechanical impedance by growing them through agar media in plates placed at a vertical orientation. Two agar concentrations, 1.2% and 2.4%, were used to provide two distinct levels of constant mechanical impedance. The lengths of wild type, *eb1b-1* mutant, and EB1b OX roots were measured while growing within media containing one of these agar concentrations. Roots of all three genotypes grown in 2.4% agar were shorter than their counterparts grown in 1.2% agar (Student's t-test, $p<0.0061$) (Figure 3.10). Lijima et al. (1991) and Materechera et al. (1991) have reported similar results, showing that the roots of various crop plants growing through media of higher density are shorter than roots growing through media of lower density. I also found that there was no significant difference between the lengths of wild type and *eb1b-1* mutant roots growing through either 1.2% or 2.4% agar (Student's t-test, $p>0.50$), indicating that the loss of EB1b has no effect on the overall elongation rates of roots growing in the presence of constant mechanical impedance and gravity. EB1b OX roots, on the other hand, were significantly shorter than both wild type and e*b1b-1* mutants growing in either of the two agar concentrations (Student's t-test, $p<0.02$), indicating that excessive amounts of EB1b have an inhibitory effect on overall root elongation rates.

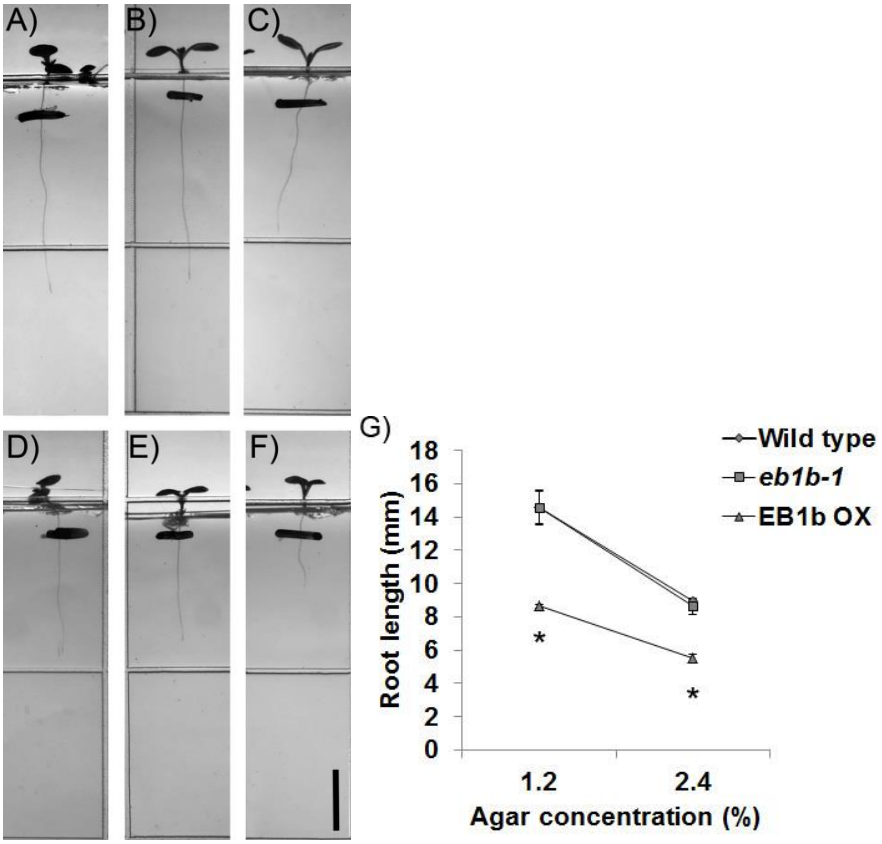

Figure 3.10 Root elongation is correlated with the level of constant mechanical impedance

Wild type (A, D), *eb1b-1* mutant (B, E), and EB1b OX (C, F) seedlings were grown vertically through either 1.2% (A, B, C) or 2.4% (D, E, F) agar for seven days. The black mark across each root indicates the root tip position on the third day of growth. Root lengths were measured along the roots from the black mark to the root tip. The size bar in (F) represents 5 mm and applies to all photographs. Data points in (G) represent averages of root length of three biological replications with standard errors. A range of 11 to 35 roots were measured per genotype in each replicate for a total of 51 to 81 roots per genotype at each agar concentration. Significantly shorter root lengths (denoted by asterisks) were observed for all three genotypes when grown in 2.4% agar compared to 1.2% agar (Student's t-test, $p<0.0061$). EB1b OX roots were significantly shorter (Student's t-test, $p<0.02$) than either wild type or *eb1b-1* mutant roots, which did not differ significantly from each other (Student's t-test, $p>0.50$) when grown in media of the same agar concentration.

Chapter 4 Discussion

Plus-end tracking proteins (+TIPs) are unique microtubule-associated proteins that specifically accumulate at growing microtubule plus-ends. EB1b, one of these +TIPs, has been shown to play a role as a repressor of root responses to a combination of gravity and transient mechanical stimulation (Bisgrove et al., 2008; Gleeson et al., 2012; Squires, 2013; this thesis). However, the mechanism by which EB1b acts as a repressor is still unknown. In my research, I created transgenic *eb1b-1* mutants carrying truncated versions of EB1b and analyzed their roots to gain insights into the mechanism by which EB1b regulates root responses to such stimulation. To do this, I created genetic constructs encoding truncated versions of EB1b, and used these constructs to generate *eb1b-1* mutant plants expressing the truncated versions of EB1b. I generated a total of six such genetic constructs. One construct had a deletion of the N-terminal microtubule-binding domain, while two other constructs had different sized deletions of the C-terminal protein-protein interaction domain. The remaining three EB1b genetic constructs that I created encode GFP fusions to each of the three EB1b deletion constructs described above. All six constructs were introduced into the genome of *Arabidopsis eb1b-1* mutants by *Agrobacterium*-mediated plant transformation. Homozygous lines carrying single (or tightly linked) transgenes were obtained. At least three lines of transgenic plants for each of the six deletion constructs were found that segregated three hygromycin resistant to one hygromycin sensitive in the T_1 generation. Of these, a range of one to five homozygous lines expressing each of the EB1bΔC1, EB1bΔC2, and EB1bΔN constructs were found. All of these transgenic *Arabidopsis* lines have been passed on to Hae Ryoung Kim, the student who will continue with this project. Mutant lines expressing the EB1bΔC2 deletion were analyzed. This truncated version of EB1b is missing the complete tail domain, to disrupt its protein-protein interaction ability (Figure 4.1C). By examining root behaviour, I found that roots of EB1bΔC2 plants behaved like *eb1b-1* plants, failing to show normal responses to a combination of gravity and transient mechanical stimulation. This finding indicates that

the ability of EB1b to modulate root responses to such cues most likely involves interactions with other cellular components.

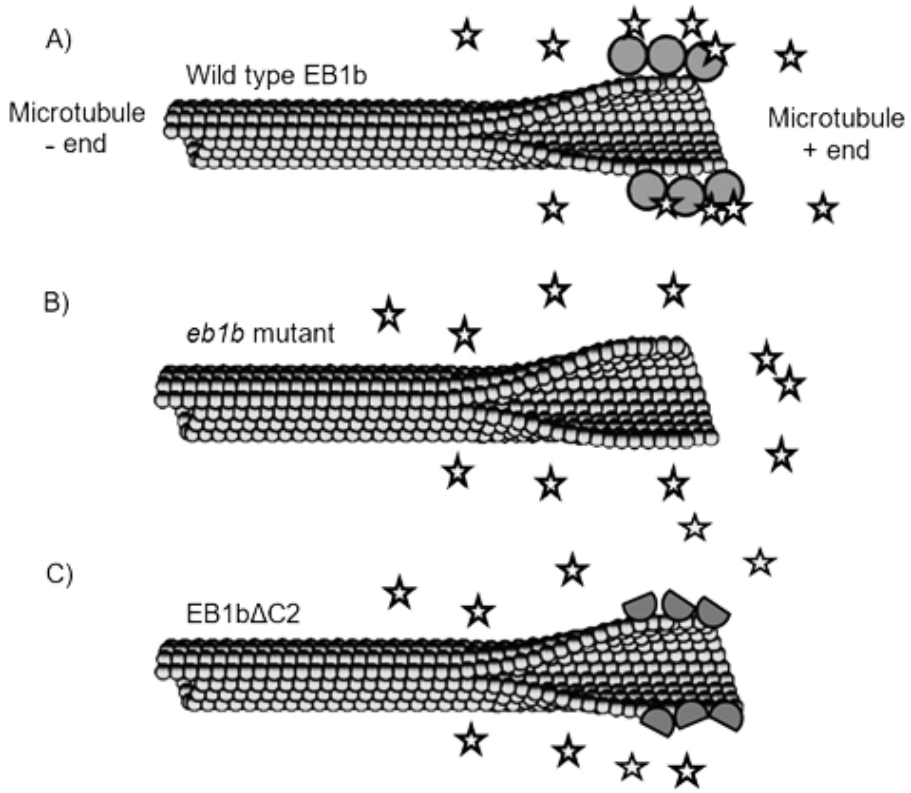

Figure 4.1 Proposed interactions between the EB1b protein and other cellular molecules in wild type, *eb1b-1*, and EB1bΔC2 *Arabidopsis* plants

(A) In wild type *Arabidopsis* plants, EB1b proteins (circles) bind to the "+" ends of microtubules via their N-terminal calponin homology domains. The C-terminal EB homology and tail domains are involved in the binding of other non-tubulin cellular molecules (stars). (B) In *eb1b-1* mutant *Arabidopsis* plants, functional EB1b proteins do not exist to bind to microtubules or other cellular molecules. (C) In EB1bΔC2 *Arabidopsis* plants, the EB1b proteins (semi circles) have a functional N-terminal calponin homology domain and thus are able to bind to microtubules, but lack their C-terminal tail domain. This domain is believed to comprise a large part of the interaction site for other cellular molecules. As such, the truncated EB1b protein in these plants is unable to interact with its usual cellular binding partners.

To understand further how EB1b functions, I investigated whether EB1b modulates root responses to gravitational and transient mechanical stimulation by affecting root skewing angle and/or elongation rates. I found that *eb1b-1* mutant roots respond to such stimulation more than the wild type roots, and that the EB1b OX roots respond less than wild type roots. These findings would suggest that EB1b plays an inhibitory role in the response to the combination of gravitational and transient

mechanical stimulation, which is in agreement with previous studies carried out by our lab (Squires, 2013; Bisgrove et al., 2008; Gleeson et al., 2012). Despite the difference in skewing angle between the *eb1b-1* mutant and wild type roots in their response to the gravitational/transient mechanical stimulation, there was no difference in root elongation rate between these two genotypes when provided with gravitational/transient mechanical cues. This result would suggest that EB1b does not regulate root responses to this type of stimulation through alteration of the root elongation rate. However, examination of root length in the EB1b OX genotype exposed to a combination of gravitational and transient mechanical stimulation revealed roots that were shorter than those seen in either wild type or the *eb1b-1* mutant plants. Thus, it would appear that EB1b can have negative effects on root elongation, but only when it is overexpressed. The protein does not appear to have a role in setting the overall rates of elongation in roots with respect to the density of the growth media. I propose that EB1b may be part of a signaling pathway that alters cell elongation in roots responding to such cues as the root grows.

In my studies, I investigated whether EB1b modulates root responses to mechanical stimulation through regulation of the root elongation rate. I assessed root elongation rates of plants expressing different levels of EB1b when exposed to transient mechanical stimulation and constant mechanical impedance. I found that the roots of all three genotypes of *Arabidopsis* (wild type, the *eb1b-1* mutant, and the overexpressor EB1b OX) were shorter when growing through media of higher densities, regardless of the presence, absence, or level of EB1b. This finding indicates that EB1b is not part of the mechanism that sets overall root elongation rates in accordance with the surrounding media. Another finding from this study also supports this idea. The loss of EB1b does not appear to affect overall root elongation rates when exposed to different levels of transient mechanical stimulation. Thus the mechanism by which overall root elongation rates are set appears to be uncoupled from the mechanism that controls root responses to transient mechanical stimulation, and appears to be regulated independently of EB1b.

Although there was no difference in root lengths, *eb1b-1* mutants had roots that skewed more than wild type when they were given transient mechanical stimulation (Gleeson et al., 2012; Squires, 2013; Bisgrove et al., 2008; this thesis). Based on this observation, EB1b is considered to be a repressor of root responses to this type of stimulation. On plates reclined from a vertical position, wild type roots normally grow

downward and encounter the agar surface. If roots are not able to penetrate into the agar, the force generated in the elongation zone causes roots to buckle. This buckling leads to a displacement of the root tip such that it is no longer parallel with the gravity vector. A bend is then formed at the base of the elongation zone that allows the root tip to reorient back into a downward growing position. It has been proposed that EB1b plays a role in formation of this downward bending in roots upon gravitropic stimulation (Squires, 2013). This idea is supported by the fact that EB1b plays a role in enhancing gravitropic responses, as shown by Gleeson et al. (2012). In their study, these authors demonstrated that *eb1b-1* mutant roots placed on their sides exhibited delays in their response to gravity. Delays in gravitropic bend formation have also been reported for *eb1b-1* mutant roots navigating around a barrier on the agar surface (Bisgrove et al., 2008). Hence, when *eb1b-1* mutant roots were stimulated with a combination of gravitational and transient mechanical cues, the disoriented roots formed a downward bend at a slower rate than that seen in the roots of wild type plants.

To understand further how EB1b functions in bend formation of roots upon touch/gravity stimulation, I assessed root behaviour in an EB1b overexpressing line (EB1b OX). In contrast to *eb1b-1* mutants, roots of the overexpressing line skewed less than wild type when stimulated with gravitational/transient mechanical cues. I also found that overexpressing EB1b results in shorter roots than those seen in either wild type or *eb1b-1* mutants. This finding held true when roots were exposed to different levels of transient mechanical stimulation or grew through different densities of media (constant mechanical stimulation). I propose that EB1b has a repressive effect on cell expansion in the elongation zone of roots, but only after exposure to transient stimulation. This repressive effect of EB1b could modulate the signaling pathways that control transient differences in cell elongation rates across the root that are needed for root bending.

It is possible that EB1b has an effect on the regulation of auxin flow. The plant hormone auxin is a key regulator of many root developmental processes, including root elongation and bend formation. How auxin affects root growth is concentration-dependent, and either increases or decreases from a basal concentration can promote or inhibit elongation, depending on the final auxin concentration (Barbier-Brygoo et al., 1991; Evans et al., 1994; Ljung et al., 2005; Rashotte et al., 2000). Upon gravitropic stimulation of a wild type root, more auxin accumulates at the lower flank of the root,

while less auxin occurs at the upper flank. This differential distribution of auxin leads to an inhibition of cell elongation in the lower flank, and a promotion of cell elongation in the upper flank (Evans et al., 1994). One possibility is that EB1b could be acting in a signaling pathway that regulates the levels of auxin flowing to the cells in the elongation zone of roots. This idea is supported by the observations that roots become shorter than wild type when EB1b is overexpressed (this thesis) and that *eb1b-1* mutant roots have delayed gravitropic responses (Gleeson et al., 2012).

EB1b also affects membrane trafficking activities inside the cell, including endocytosis (Shahidi, 2013). Thus, it is possible that upregulation or loss of EB1b activity could lead to changes in the amount of auxin transporters being placed on the membrane or affect how well these proteins translocate from one side of the cell to another. In response to stimulation, the allocation of auxin transporters is mediated by membrane trafficking, where these proteins are recycled between the membrane compartments within the cell or translocated to a different side of the cell. The membrane-bound auxin transporters AUXIN RESISTANT 1 (AUX1) influx and PIN FORMED (PIN) are the primary regulators of auxin flow in plants (Bennett et al., 1996; Galweiler et al., 1998; Muller et al., 1998). Distribution of these auxin transporters at the polar ends of a cell directs the flow of auxin (Wisniewska et al., 2006). Local auxin concentrations in roots can then be established by the movement of auxin from cell to cell. As such, differential auxin concentrations along the flanks of roots would take much longer to become established in *eb1b-1* mutants, creating the delay in responses to gravity stimulation observed in these roots. Given the role of auxin and differential auxin transport in root elongation (Blilou et al., 2005), this type of EB1b-induced disturbances in differential auxin concentrations could reduce cell expansion in the elongation zone of the root, ultimately explaining the shorter roots observed in the EB1b overexpressing line EB1b OX.

Previous studies carried out in our laboratory have shown that another player, TCH3, enhances root responses to transiently applied mechanical stimuli (Gleeson et al., 2012). TCH3 is a calmodulin-like calcium binding protein that participates in calcium-mediated signal transduction and is transcriptionally activated in response to mechanical cues (Braam and Davis, 1990). Insertional mutants of *TCH3* show a decreased response to mechanical stimuli compared to that seen in wild type plants, while *eb1b-1*

mutants show an increased response to mechanical stimulation (Bisgrove et al., 2008). Double mutants display a root response that is indistinguishable from that seen in wild type plants. Taken together, these results led the authors of this study to suggest that the hypersensitivity of *eb1b-1* mutants to mechanical cues is due to the resulting unrepressed TCH3 activity (Gleeson et al., 2012).

It has also been shown that actin filaments from root cells of *eb1b-1* mutant plants are more stable than those from wild type plants. Apparently, EB1b has a destabilizing effect on these cytoskeletal components (Shahidi, 2013). Based on his findings, this author proposed that EB1b plays a role in maintaining a proper balance of actin polymerization and depolymerisation within *Arabidopsis* root cells.

Exactly how the cellular activities of EB1b influence root responses to the combination of gravitational and transient mechanical stimulation is still largely unknown. Based on all of the above evidence, I propose the following model to account for the activities of this protein. The activation of TCH3 in response to the plant's perception of such stimuli results in changes to the membrane trafficking of auxin transporters, ultimately giving rise to changes in auxin movement within the root. Such changes in the transport of auxin would in turn result in changes to cell expansion rates within the elongation zone of the root. Given that *eb1b-1* mutants exhibit slower gravitropic responses, indicating that they are slower to alter cell expansion rates across the root, it would appear that EB1b inhibits this pathway (Figure 4.2).

It is also apparent that EB1b inhibits root elongation, at least when it is overexpressed. (Recall that EB1b OX roots were shorter than either wild type or *eb1b-1* mutant roots.) If EB1b has the same effect in wild type roots that are forming a bend in response to touch/gravity cues, this would induce a decrease in cell elongation on the inner (or shorter) flank of the bending root (i.e., the lower side of a root that is responding to gravity). The slower response of *eb1b-1* mutant roots to touch/gravity stimulation could be explained in this way, as the mutant roots are not able to establish a pronounced differential growth rate between the cells of upper and lower flanks as quickly as the wild type roots because the inhibitory effects of EB1b are missing. Increases in the time taken to form such downward bends also accounts for the

increased skewing angles measured in *eb1b-1* mutant roots in response to gravitational/transient mechanical stimuli on reclined agar plates.

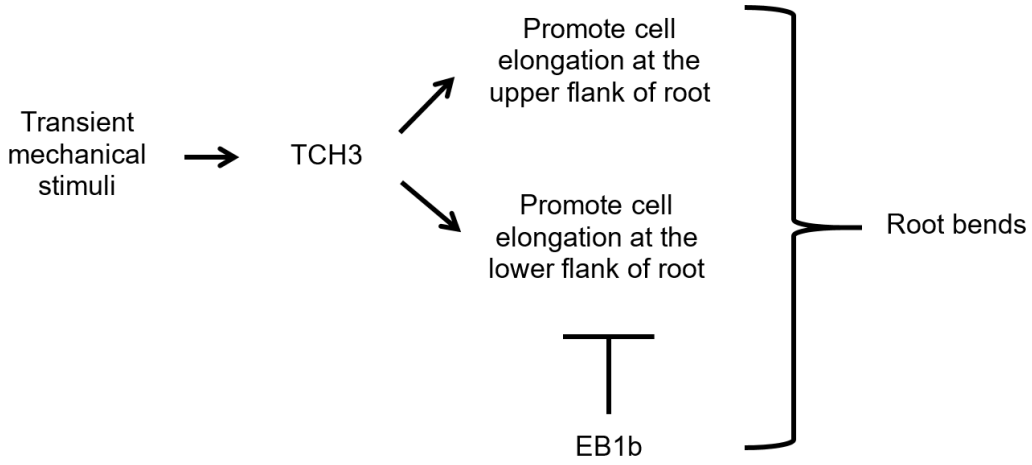

Figure 4.2 Model of EB1b action in *Arabidopsis* roots upon transient mechanical stimulation

When *Arabidopsis* roots perceive transient mechanical stimulation, TCH3, a calmodulin-like protein, becomes activated. In its active form, TCH3 promotes cell expansion within the elongation zone of the root on both upper and lower root flanks. The resulting increase in cell elongation could take place via changes to the membrane trafficking of auxin transporters, ultimately resulting in changes to auxin movement within the root. EB1b acts to inhibit elongation in the lower, but not the upper, root flank. The resulting differential growth rates on opposing root flanks result in the formation of a bend in the growing root.

To investigate how EB1b functions in response to mechanical stimulation at a more molecular level, I examined the behaviour of transgenic *eb1b-1* mutant roots expressing EB1bΔC2 deletion constructs in response to gravitational/transient mechanical stimuli. The protein encoded by the EB1bΔC2 deletion construct is missing the amino acids from the C-terminus that make up the tail domain. I found that transgenic *eb1b-1* mutant roots skewed leftward in a manner equivalent to untransformed mutants and significantly more than wild type. These results suggest that EB1b interactions with other non-tubulin proteins are likely required for normal regulation of root responses to such cues. In a 2013 study by Squires, *eb1b-1* mutant plants transformed with a full length EB1b-GFP fusion construct also had skewing phenotypes equivalent to untransformed *eb1b-1* mutants. Since this construct was able to bind microtubules normally, it was suspected that the GFP moiety might be interfering with the functions of the C-terminus of EB1b. My results provide further evidence that the C-terminus of EB1b is indeed required for normal regulation of root responses to transient

mechanical stimulation. The C-terminus of EB1 serves as a major binding surface for cellular components (Figure 4.1). In its homodimeric form, the tail region of EB1, together with a coiled coil region in the EB homology domain, forms a unique four-helix bundle motif (Slep et al., 2005). This four helix bundle in the C-terminus forms a binding pocket for EB1 interactors. The deletion of the EB1b tail removes a large portion of this binding pocket (i.e., two of the four alpha helices), which likely renders the protein unable to provide proper molecular complementarity for its interacting partner(s).

The exact binding partner(s) of EB1b in *Arabidopsis* is still unknown. Studies of EB1 in animals have shown that this family of proteins can interact with a diverse array of cellular molecules, including components of signaling cascades, membrane trafficking complexes, actin-associated proteins, and other microtubule associated proteins (Jiang et al., 2012). Therefore, based on the work of these researchers, and the high degree of conservation of this protein, it is possible that in *Arabidopsis*, EB1b is interacting with a kinase or phosphatase that is activated by the TCH3 signaling cascade, with GTPases or their effectors that are components of membrane trafficking complexes, or with other proteins that bind to either actin filaments or microtubules, perhaps affecting the stability of these cytoskeletal components. Such effects on cytoskeletal dynamics could change cell expansion rates in response to an incoming signal by affecting the rate at which the signal (associated with the + end) is delivered to the appropriate subcellular site.

Chapter 5 Conclusions and Future Directions

The aim of my research for this thesis was to understand how EB1b modulates root responses to mechanical stimulation. Through the studies I have described herein, I have found that 1) EB1b regulates root responses to transient mechanical stimuli, but is not involved in the mechanism determining overall root elongation rates based on the density of the growth medium (i.e., constant mechanical cues); 2) when present at higher than normal levels, EB1b has an inhibitory effect on root elongation, suggesting that this protein can reduce cell expansion in the elongation zone of the root; and 3) the C-terminal protein-protein interaction domain of EB1b is required for the regulation of root responses to transient mechanical cues.

I propose the following model to account for the activities of EB1b in *Arabidopsis* roots. Upon perception of transient mechanical cues, the plant activates TCH3, which results in changes to the membrane trafficking of auxin transporters, ultimately giving rise to localized changes in auxin concentrations within the root. Such changes in the concentrations of this phytohormone would in turn result in changes to cell expansion rates within the elongation zone of the root. EB1b seems to inhibit this pathway.

We know that EB1 family members accumulate at the plus end of microtubules through their N-terminal calponin domain. While bound to microtubules, EB1 members can also influence microtubule dynamics, likely through interactions with other proteins (Komaki et al., 2010; Hayashi et al., 2005). Whether or not EB1b affects root responses to touch/gravity stimulation by binding to microtubules and influencing microtubule dynamics is a question that can be answered using the EB1b N-terminal truncation line of *Arabidopsis* (EB1bΔN) that I created. If the roots of EB1bΔN show the same response as the roots of the untransformed *eb1b-1* mutant when grown on reclined agar plates, then we know that EB1b binding to microtubules is required for cellular responses to such cues.

The exact binding partner(s) of EB1b in the *Arabidopsis* root response to mechanical stimulation are still unknown. These proteins could be isolated using a pull-down assay with EB1b as the "bait" protein. Tagged, bead-immobilized EB1b could be incubated with lysates taken from root tissue exposed to transient mechanical stimulation. Proteins of interest could be eluted from the beads using a series of washes, with the eluted proteins being collected by centrifugation, and then analysed by SDS-PAGE. Protein bands could be isolated from the gel, and the proteins contained therein identified using mass spectrometry or protein sequencing.

So far, we have found that EB1b plays a role in gravitropism and in responses to transient combinations of touch/gravity cues. It would be interesting to determine if it is involved in other types of root responses to transient stimulation (e.g., hydrotropism, halotropism, or thermotropism). This could be accomplished by comparing the responses seen in both wild type and *eb1b-1* mutant *Arabidopsis* plants upon exposure to the appropriate stimuli. Assuming that EB1b is found to be involved in another of these "tropisms", the EB1b overexpressor (EB1b OX) could be used, as could the truncated EB1b mutant *Arabidopsis* lines that I generated for my studies (EB1bΔN, EB1bΔC1, and EB1bΔC2) to investigate the role of expression levels and the various domains of EB1b, respectively, in this response.

Thus, EB1bΔN, EB1bΔC1, and EB1bΔC2 have great potential to assist with the elucidation of cellular/molecular mechanisms of EB1b action in future studies carried out in our laboratory. Furthermore, EB1b[ΔN]-GFP, EB1b[ΔC1]-GFP, and EB1b[ΔC2]-GFP allow for the three truncated versions of EB1b to be tracked within cells, to determine if their localization patterns differ from that of wild type EB1b. One current project, examining the role of EB1b in root hair development, is already in progress, with the aid of these six truncated EB1b *Arabidopsis* lines.

References

Akbari, O. S., Oliver, D., Eyer, K., and Pai, C. (2009). An Entry/Gateway® cloning system for general expression of genes with molecular tags in *Drosophila melanogaster*. BioMed Central Cell Biology 10:8. doi:10.1186/1471-2121-10-8.

Alberti, S., Gitler, A. D., and Lindquist, S. (2007). A suite of Gateway® cloning vectors for high-throughput genetic analysis in *Saccharomyces cerevisiae*. National Institute of Health *24*, 913-919.

Arioli, T., Peng, L., Betzner, A. S., Burn, J., Wittke, W., Herth, W., Camilleri, C., Hofte, H., Plazinski, J., Birch, R., Cork, A., Glover, J., Redmond, J., and Williamson, R. E. (1998). Molecular analysis of cellulose biosynthesis in *Arabidopsis.* Science *279*, 717-720.

Barbier-Brygoo, H., Ephritikhine, G., Klambt, D., Maurel, C., Palme, K., Schell, J., and Guern, J. (1991). Perception of the auxin signal at the plasma membrane of tobacco mesophyll protoplasts. The Plant Journal *1*, 83-93.

Barton, K. A., Binns, A. N., Matzke, A. J. M., and Chilton, M. (1983). Regeneration of intact tobacco plants containing full length copies of genetically engineered T-DNA, and transmission of T-DNA to R1 progeny. Cell *32,* 1033-1043.

Baskin, T. (2001). On the alignment of cellulose microfibrils by cortical microtubules: a review and a model. Protoplasma *215*, 150-170.

Baskin, T. I., Wilson, J. E., Cork, A., and Williamson, R. E. (1994). Morphology and microtubule organization in *Arabidopsis* roots exposed to oryzalin or taxol. Plant Cell Physiology *35*, 935-942.

Bates, T. R. and Lynch, J. P. (1996). Stimulation of root hair elongation in Arabidopsis thaliana by low phosphorus availability. Plant, Cell and Environment *19*, 529-538.

Bechtold, N. and Pelletier, G. (1998). *In planta Agrobacterium*-mediated transformation of adult *Arabidopsis thaliana* plants by vacuum infiltration. Methods in Molecular Biology *82*, 259-266.

Beetham, P. R., Kipp, P. B., Sawycky, X. L., Arntzen, C. J., and May, G. D. (1999). A tool for functional plant genomics: chimeric RNA/DNA oligonucleotides cause in vivo gene-specific mutations. Proceedings of the National Academy of Sciences *96*, 8774-8778.

Bennett, M. J., Marchant, A., Green, H. G., May, S. T., Ward, S. P., Milner, P. A., Walker, A. R., Schulz, B., and Feldmann, K. A. (1996). Arabidopsis AUX1 gene: a permease-like regulator of root gravitropism. Science *273*, 948-950.

Bermingham, N. and Luettich, K. (2003). Polymerase chain reaction and its applications. Current Diagnostic Pathology *9*, 159-164.

Bisgrove, S. R. (2011). Microtubules and root responses to mechanical impedance and gravity. The Americas Journal of Plant Science and Biotechnology *5*, 98-106.

Bisgrove, S. R., Hable, W. E., and Kropf, D. L. (2004). +TIPs and microtubule regulation. The beginning of the plus end in plants. Plant Physiology *136*, 3855-3863.

Bisgrove, S. R., Lee, Y. J., Liu, B., Peters, N. T., Kropf, D. L. (2008). The microtubule plus-end binding protein EB1 functions in root responses to touch and gravity signals in *Arabidopsis*. The Plant Cell *20*, 396-410.

Blilou, I., Xu, J., Wildwater, M., Willemsen, V., Paponov, I., Friml, J., Heidstra, R., Aida, M., Palme, K., and Scheres, B. (2005). The PIN auxin efflux facilitator network controls growth and patterning in *Arabidopsis* roots. Nature *433*, 39-44.

Braam, J. and Davis, R. W. (1990). Rain-, wind-, and touch-induced expression of calmodulin and calmodulin-related genes in Arabidopsis. Cell *60*, 357-364.

Brand, L., Horler, M., Nuesch, E., Vassalli, S., Barrell, P., Yang, W., Jefferson, R. A., Grossniklaus, U., and Curtis, M. D. (2006). A versatile and reliable two-component system for tissue-specific gene induction in *Arabidopsis*. Plant Physiology *141*, 1194-1204.

Braun, A. (1947). Thermal studies on the factors responsible for tumor initiation in crown gall. American Journal of Botany *34*, 234-240.

Bu, W. and Su, L. (2003). Characterization of functional domains of human EB1 family proteins. The Journal of Biological Chemistry *278*, 49721-49731.

Burk, D. H. and Ye, Z. H. (2002). Alteration of oriented deposition of cellulose microfibrils by mutation of a katanin-like microtubule-severing protein. The Plant Cell *14*, 2145-2160.

Chalfie, M., Tu, Y., Euskirchen, G., Ward, W. W., and Prasher, D. C. (1994). Green florescent protein as a marker for gene expression. Science *263*, 802-805.

Chan, J., Calder, G. M., Doonan, J. H., and Lloyd, C. W. (2003). EB1 reveals mobile microtubule nucleation sites in *Arabidopsis*. Nature Cell Biology *5*, 967-971.

Chang, S. S., Park, S. K., Kim, B. C., Kang, B. J., Kim, D. U., and Nam, H. G. (1994). Stable genetic transformation on *Arabidopsis thaliana* by *Agrobacterium* inoculation *in planta*. The Plant Journal *5*, 551-558.

Chilton, M-D., Drummond, M. H., Merlo, D. J., Sciaky, D., Montoya, A. L., Gordon, M. P., and Nester, E. W. (1977). Stable incorporation of plasmid DNA into higher plant cells: the molecular basis of crown gall tumorigenesis. The Cell *11*, 263-271.

Chumakov, M. I., Rozhok, N. A., Velikov, V. A., Tyrnov, V. S., and Volokhina, I. V. (2006). *Agrobacterium*-mediated *in planta* transformation of maize via pistil filaments. Russian Journal of Genetics *42*, 893-897.

Clough, S. J. and Bent, A. F. (1998). Floral dip: a simplified method for *Agrobacterium*-mediated transformation of *Arabidopsis thaliana.* The Plant Journal*16*, 735-743.

Coquelle, F. M., Vitre, B., and Arnal, I. (2009). Structural basis of EB1 effects on microtubule dynamics. Biochemical Society Transactions *37*, 997-1001.

Curtis, I. S. and Nam, H. G. (2001). Transgenic radish (*Raphanus sativus* L. *longipinnatus* Bailey) by floral-dip method – plant development and surfactant are important in optimizing transformation efficiency. Transgenic Research *10*, 363-371.

Curtis, M. D. and Grossniklaus, U. (2003). A Gateway cloning vector set for high-throughput functional analysis of genes *in planta*. Plant Physiology *133*, 462-469.

De Cleene, M. and De Ley, J. (1976). The host range of crown gall. Botanical Review *42*, 389-466.

de Framond, A. J., Barton, K. A., and Chilton M. (1983). Mini-Ti: a new vector strategy for plant genetic engineering. Nature Biotechnology *1*, 262-269.

Dessaux, Y., Guyon, P., Farrand, S. K., Petit, A., and Tempe, J. (1986). Agrobacterium Ti and Ri plasmids specify enzymic lactonization of mannopine to agropine. Journal of General Microbiology *132*, 2549-2559.

Ditengou, F. A., Teale, W. D., Kochersperger, P., Flittner, K. A., Kneuper, I., van der Graaff, E., Nziengui, H., Pinosa, F., Li, X., Nitschke, R., Laux, T. and Palme, K. (2008). Mechanical induction of lateral root initiation in *Arabidopsis thaliana*. Proceedings of the National Academy of Sciences *105*, 18818-18823.

Dixit, R., Barnett, B., Lazarus, J. E., Tokito, M., Goldman, Y. E., and Holzbaur, E. K. F. (2009). Microtubule plus-end tracking by CLIP-170 requires EB1. Proceedings of the National Academy of Sciences *106*, 492-497.

Dixit, R., Chang, E., and Cyr, R. (2006). Establishment of polarity during organization of the acentrosomal plant cortical microtubule array. Molecular Biology of the Cell *17*, 1298-1305.

Earley, K. W., Haag, J. R., Pontes, O., Opper, K., Juehne, T., Song, K., and Pikaard, C. S. (2006). Gateway-compatible vectors for plant functional genomics and proteomics. The Plant Journal *45*, 616-629.

El'konin, L. A., Ravin, N. V., Leshko, E. V., Volokhina, I. V., Chumakov, M. I., and Skryabin, K. G. (2009). *In planta* Agrobacterial transformation of sorghum plants. Biotekhnologiya *1*, 23-30.

Escobar, M. A. and Dandekar, A. M. (2003). *Agrobacterium tumefaciens* as an agent of disease. Trends in Plant Science *8*, 380-386.

Evans, M. L., Ishikawa, H., and Estelle, M. A. (1994). Responses of Arabidopsis roots to auxin studied with high temporal resolution: Comparison of wild type and auxin-response mutants. Planta *194*, 215-222.

Feldmann, K. A. and Marks, M. D. (1987). *Agrobacterium*-mediated transformation of germinating seeds of *Arabidopsis thaliana*: a non-tissue culture approach. Molecular and General Genetics *208*, 1-9.

Fischer, R. and Emans, N. (2000). Molecular farming of pharmaceutical proteins. Transgenic Research *9*, 279-299.

Fisher, D. D. and Cyr, R. J. (1998). Extending the microtubule/microfibril paradigm. Plant Physiology *116*, 1043-1051.

Food and Agriculture Organization of the United Nation Statistics Division (2015a). Food supply - crops primary equivalent sheet. Available at: http://faostat3.fao.org.

Food and Agriculture Organization of the United Nations (2011). The state of the world's land and water resources for food and agriculture - managing systems at risk. London: The Food and Agriculture Organization of the United Nations and Earthscan.

Food and Agriculture Organization of the United Nations Statistics Division (2015b). Global population composition by year 2050 sheet. Available at: http://faostat3.fao.org.

Food and Agriculture Organization, World Food Programme, and International Fund for Agricultural Development of the United Nations. (2014). The state of food insecurity in the world 2015. Rome: Food and Agriculture Organization.

Frandsen, R. J. N. (2011). A guide to binary vectors and strategies for targeted genome modification in fungi using *Agrobacterium tumefaciens*-mediated transformation. Journal of Microbiological Methods *87*, 247-262.

Furutani, I., Watanabe, Y., Prieto, R., Masukawa, M., Suzuki, K., Naoi, K., Thitamadee, S., Shikanai, T., and Hashimoto, T. (2000). The *SPIRAL* genes are required for directional control of cell elongation in *Arabidopsis thaliana*. Development *127*, 4443-4453.

Galjart, N. (2010). Plus-end-tracking proteins and their interactions at microtubule ends. Current Biology *20*, R528-R537.

Galva, C. Kirik, V., Lindeboom, J. J., Kaloriti, D., Rancour, D. M., Hussey, P. J., Bednarek, S. Y., Ehrhardt, D. W., and Sedbrook, J. C. (2014). The microtubule plus-end tracking proteins SPR1 and EB1b interact to maintain polar cell elongation and directional organ growth in *Arabidopsis*. Plant Cell *11*, 4409-4425.

Galvan-Ampudia, C. S., Julkowska, M. M., Darwish, E., Gandullo, J., Korver, R. A., Brunoud, G., Haring, M. A., Munnik, T., Vernoux, T., and Testerink, C. (2013). Halotropism is a response of plant roots to avoid a saline environment. Current Biology *23*, 2044-2050.

Galweiler, L., Guan, C., Muller, A., Wisman, E., Mendgen, K., Yephremov, A., Palme, K. (1998). Regulation of polar auxin transport by AtPIN1 in *Arabidopsis* vascular tissue. Science *182*, 2226-2230.

Gardiner, J. and Marc, J. (2003). Putative microtubule-associated proteins from the Arabidopsis genome. Protoplasma *222*, 61-74.

Ge, L. and Rudolph, P. (1997). Simultaneous introduction of multiple mutations using overlap extension PCR. BioTechniques *1*, 28-30.

Gehl, C., Waadt, R., Kudla, J., Mendel, R., and Hansch, R. (2009). New Gateway vectors for high throughput analyses of protein-protein interactions by bimolecular fluorescence complementation. Molecular Plant *2*, 1051-1058.

Gerdes, H. and Kaether, C. (1996). Green fluorescent protein: applications in cell biology. Federation of European Biochemical Societies Letters *389*, 44-47.

Gillooly, D. J., Morrow, I. C., Lindsay, M., Gould, R., Bryant, N. J., Gaullier, J., Parton, R. G., and Stenmark, H. (2000). Localization of phosphatidylinositol 3-phosphate in yeast and mammalian cells. The EMBO Journal *19*, 4577-4588.

Gleeson, L., Squires, S., and Bisgrove, S. R. (2012). The microtubule associated protein END BINDING 1 represses root responses to mechanical cues. Plant Sciences *187*, 1-9.

Green, P. B. (1962). Mechanism for plant cellular morphogenesis. Science *138*, 1404-1405.

Gu, C., Zhou, W. Puthenveedu, M. A., Xu, M., Jan, Y. N., and Jan, L. Y. (2006). The microtubule plus-end tracking protein EB1 is required for Kv1 voltage-gated K^+ channel axonal targeting. Neuron *52*, 803-816.

Haberlandt, G. (1914). Physiological plant anatomy. Translated by Drummond, M. London: Macmillan and Co. Limited.

Hagelberg, E. (1991). Polymerase chain reaction - technology and applications. Analytical Proceedings *28*, 152-155.

Hamilton, E. S., Schlegel, A. M., and Haswell, E. S. (2015). United in diversity: mechanosensitive ion channels in plants. Annual Review of Plant Biology *66*, 8.1-8.25.

Hayashi, I. and Ikura, M. (2003). Crystal structure of the amino-terminal microtubule-binding domain of End-binding Protein 1 (EB1). The Journal of Biological Chemistry *278*, 36430-36434.

Hayashi, I., Wilde, A., Mal, T. K., and Ikura, M. (2005). Structural basis for the activation of microtubule assembly by the EB1 and $p150^{Glued}$ complex. Molecular Cell *19*, 449-460.

Hellens, R. and Mullineaux, P. (2000). A guide to *Agrobacterium* binary Ti vectors. Trends in Plant Sciences *5*, 446-451.

Higuchi, R., Krummel, B., and Saiki, R. (1988). A general method of *in vitro* preparation and specific mutagenesis of DNA fragments: study of protein and DNA interactions. Nucleic Acid Research *16*, 7351-7367.

Himmelbach, A., Zierold, U., Hensel, G., Riechen, J., Douchkov, D., Schweizer, P., and Kumlehn, J. (2007). A set of modular binary vectors for transformation of cereals. Plant Physiology *145*, 1192-1200.

Himmelspach, R., Williamson, R. E., and Wasteneys, G. O. (2003). Cellulose microfibril alignment recovers from DCB-induced disruption despite microtubule disorganization. The Plant Journal *36*, 565-575.

Hoekema, A., Hirsch, P. R., Hooykaas, P. J. J., and Schilperoort, R. A. (1983). A binary plant vector strategy based on separation of *vir*- and T-region of *the Agrobacterium tumefaciens* Ti-plasmid. Nature *303*, 179-180.

Honnappa, S., John, C. M., Kostrewa, D., Winkler, F. K., and Steinmetz, M. O. (2005). Structural insights into the EB1-APC interaction. The EMBO Journal *24*, 261-269.

Honnappa, S., Gouveia, S. M., Weisbrich, A., Damberger, F. F., Bhavesh, N. S., Jawhari, H., Grigoriev, I., van Rijssel, F. J. A., Buey, R. M., Lawera, A., Jelesarov, I., Winkler, F. K., Wuthrich, K., Akhmanova, A., and Steinmetz, M. O. (2009). An EB1-binding motif acts as a microtubule tip localization signal. Cell *138*, 366-376.

Huala, E., Dickerman, A. W., Garcia-Hernandez, M., Weems, D., Reiser, L., LaFond, F., Hanley, D., Kiphart, D., Zhuang, M., Huang, W., Mueller, L. A., Bhattacharyya, D. B., Bhaya, D., Sobral, B. W., Beavis, W., Meinke, D. W., Town, C. D., Somerville, C., and Rhee, S. Y. (2001). The Arabidopsis Information Resource (TAIR): a comprehensive database and web-based information retrieval, analysis, and visualization system for a model plant. Nucleic Acids Research *29*, 102-105.

Hutchison, C. A. 3rd, Phillips, S., Edgell, M. H., Gillam, S., Jahnke, P., and Smith, K. (1978). Mutagenesis at a specific position in a DNA sequence. Journal of Biological Chemistry *253*, 6551-6560.

Inouye, S. and Tsuji, F. I. (1994). *Aequorea* green fluorescent protein: expression of the gene and fluorescence characteristics of the recombinant protein. Federation of European Biochemical Societies Letters *341*, 277-280.

Ishida T. and Hashimoto, T. (2007). An *Arabidopsis thaliana* tubulin mutant with conditional root-skewing phenotype. Journal of Plant Research *120*, 635-640.

Jiang, K., Toedt, G., Gouveia, S. M., Davey, N. E., Hua, S., van der Vaart, B., Grigoriev, I., Larsen, J., Pedersen, L. B., Bezstarosti, K., Lince-Faria, M., Demmers, J., Steinmetz, M. O., Gibson, T. J., and Akhmanova, A. (2012). A proteome-wide screen for mammalian SxIP motif-containing microtubule plus-end tracking proteins. Current Biology *22*, 1800-1807.

Jin, S., McKee, T. D., and Oprian, D. D. (2003). An improved rhodopsin/EGFP fusion protein for use in the generation of transgenic *Xenopus laevis.* Federation of European Biochemical Societies Letters *542*, 142-146.

Katavic, V., Haughn, G. W., Reed, D., Martin, M., and Kunst, L. (1994). *In planta* transformation of *Arabidopsis thaliana*. Molecular Genetics and Genomics *245*, 363-370.

Kempin, S. A., Liljegren, S. J., Block, L. M., Rounsley, S. D., Yanofsky, M. F., and Lam, E. (1997). Targeted disruption in *Arabidopsis*. Nature *389*, 802-803.

Kim, K. and Farrand, S. K. (1996). Ti plasmid-encoded genes responsible for catabolism of the crown gall opine mannopine by *Agrobacterium tumefaciens* are homologs of the T-region genes responsible for synthesis of this opine by the plant tumor. Journal of Bacteriology *178*, 3275-3284.

Kim, K., Baek, C-H., Lee, J., Yang, J. M., and Farrand, S. K. (2001). Intracellular accumulation of mannopine, and opine produced by crown gall tumors, transiently inhibits growth of *Agrobacterium tumefaciens*. Molecular Plant-Microbe Interactions *14*, 793-803.

Kimbrough, J. M., Salinas-Mondragon, R. S., Boss, W. F., Brown, C. S., and Sederoff, H. W. (2004). The fast and transient transcriptional network of gravity and mechanical stimulation in the *Arabidopsis* root apex. Plant Physiology *136*, 2790-2805.

Kiss, J. Z., Wright, J. B., and Caspar, T. (1996). Gravitropism in roots of intermediate-starch mutants of *Arabidopsis*. Physiologia Plantarum *97*, 237-244.

Klusener, B. and Weiler, E. W. (1999). A calcium-sensitive channel from root-tip endomembranes of garden cress. Plant Physiology *119*, 1399-1405.

Komaki, S., Abe, T., Coutuer, S., Inze, D., Russinova, E., and Hashimoto, T. (2010). Nuclear-localized subtype of end-binding 1 protein regulates spindle organization in *Arabidopsis*. Journal of Cell Science *123*, 451-459.

Komarova, Y., De Groot, C. O., Grigoriev, I., Gouveia, S. M., Munteanu, E. L., Schober, J. M., Honnappa, S., Buey, R. M., Hoogenraad, C. C., Dogterom, M., Barisy, G. G., Steinmetz, M. O., and Akhmanova, A. (2009). Mammalian end binding proteins control persistent microtubule growth. Journal of Cell Biology *184*, 691-706.

Komori, T., Imayama, T., Kato, N., Ishida, Y., Ueki, J., and Komari, T. (2007). Current status of binary vectors and superbinary vectors. Plant Physiology *145*, 1155-1160.

Koornneef, M. and Meinke, D. (2010). The development of *Arabidopsis* as a model plant. The Plant Journal *61*, 909-921.

Kurusu, T., Yamanaka, T., Nakano, M., Takiguchi, A., Ogasawara, Y., Hayashi, T., Iida, K., Hanamata, S., Shinozaki, K., Iida, H., and Kuchitsu, K. (2012). Involvement of the putative Ca^{2+}-permeable mechanosenstitive channels, in Ca^{2+} uptake, Ca^{2+}-dependent cell proliferation and mechanical stress-induced gene expression in tobacco (*Nicotinana tabacum*) BY-2 cells. Journal of Plant Research *125*, 555-568.

Landy, A. (1989). Dynamic, structural, and regulatory aspect of λ site-specific recombination. Annual Review of Biochemistry *58*, 913-941.

Lansbergen, G. and Akhmanova, A. (2006). Microtubule plus end: a hub of cellular activities. Traffic *7*, 499-507.

Ledbetter, M. C. and Porter, K. R. (1963). A “microtubule” in plant cell fine structure. The Journal of Cell Biology *19*, 239-250.

Leitz, G., Kang, B., Schoenwaelder, M. E. A., and Staehelin, L. A. (2009). Statolith sedimentation kinetics and force transduction to the cortical endoplasmic reticulum in gravity-sensing *Arabidopsis* columella cells. The Plant Cell *21*, 843-860.

Liakopoulos, D., Kusch, J., Grava, S., Vogel, J., and Barral, Y. (2003). Asymmetric loading of Kar9 onto spindle poles and microtubules ensures proper spindle alignment. Cell *112*, 561-574.

Lijima, M., Kono, Y., Yamauchi, A., and Pardales, J. R. Jr. (1991). Effects of soil compaction on the development of rice and maize root systems. Environment and Experimental Botany *3*, 333-342.

Liu, X., Brost, J., Hutcheon, C., Guilfoil, R., Wilson, A. K., Leung, S., Shewmaker, C. K., Rooke, S., Nguyen, T., Kiser, J., and De Rocher, J. (2012). Transformation of the oilseed crop *Camelina sativa* by *Agrobacterium*-mediated floral dip and simple large-scale screening of transformants. In Vitro Cellular & Developmental Biology - Plant *48*, 462-468.

Ljung, K., Bhalerao, R. P., and Sandberg, G. (2001). Sites and homeostatic control of auxin biosynthesis in *Arabidopsis* during vegetative growth. The Plant Journal *28*, 465-474.

Ljung, K., Hull, A. K., Cleneza, J., Yamada, M., Estelle, M., Normanly, J., and Sandberg, G. (2005). Sites and regulation of auxin biosynthesis in Arabidopsis roots. The Plant Cell *17*, 1090-1104.

Loenen, W. A. M., Dryden, D. R. F., Raleigh, E. A., Wilson, G. G., and Murray, N. E. (2013). Highlights of the DNA cutters: a short history of the restriction enzymes. Nucleic Acids Research *42*, 1-17.

Lyi, S. M., Jafri, S., and Winans, S. C. (1999). Mannopinic acid and agropinic acid catabolism region of the octopine-type Ti plasmid pTi15955. Molecular Microbiology *31*, 339-347.

MacCleery, S. A. and Kiss, J. Z. (1999). Plastid sedimentation kinetics in roots of wild-type and starch-deficient mutants of *Arabidopsis*. Plant Physiology *120*, 183-192.

Manna, T., Honnappa, S., Steinmetz, M. O., and Wilson, L. (2008). Suppression of microtubule dynamic instability by the +TIP protein EB1 and its modulation by the CAP-Gly domain of $p150^{Glued}$. Biochemistry *47*, 779-786.

Martinac, B., Buechner, M., Delcour, A. H., Adler, J., and Kung, C. (1987). Pressure-sensitive ion channel in *Escherichia coli*. Proceedings of the National Academy of Sciences *84*, 2297-2301.

Massa, G. D. and Gilory, S. (2003). Touch modulates gravity sensing to regulate the growth of primary roots of *Arabidopsis thaliana*. The Plant Journal *33*, 435-445.

Materechera, S. A., Dexter, A. R., and Alston, A. M. (1991). Penetration of very strong soils by seedling roots of different plant species. Plant and Soil *135*, 31-41.

Mathur, J., Mathur, N., Kernebeck, B., Srinivas, B. P., and Hulskamp, M. (2003). A novel localization pattern for an EB1-like protein links microtubule dynamics to endomembrane organization. Current Biology *13*, 1991-1997.

Matz, M. V., Fradkov, A. F., Labas, Y. A., Savitsky, A. P., Zaraisky, A. G., Markelov, M. L., and Lukyanov, S. A. (1999). Florescent proteins from nonbioluminescent Anthozoa species. Nature Biotechnology *17*, 969-973.

Meagher, R. B. and Fechheimer, M. (2003). The Arabidopsis cytoskeletal genome, in Sommerville, C. R. and Meyerowitz, E. M. (ed.). The Arabidopsis Book. Rockville, MD: American Society of Plant Biologists, 1-26.

Mehta, R. K. and Singh, J. (1999). Bridge-overlap-extension PCR method for constructing chimeric genes. BioTechniques *26*, 1082-1086.

Meyer, R. S., DuVal, A. E., and Jensen, H. R. (2012). Patterns and processes in crop domestication: an historical review and quantitative analysis of 203 global food crops. New Phytologist *196*, 29-48.

Meyerowitz, E. M. (1989). *Arabidopsis*, a useful weed. Cell *56*, 263-269.

Mimori-Kiyosue, Y., Shiina, N., and Tsukita, S. (2000). The dynamic behavior of the APC-binding protein EB1 on the distal ends of microtubules. Current Biology *10*, 965-968.

Mishima, M., Maesaki, R., Kasa, M., Watanabe, T., Kukata, M., Kaibuchi, K., and Hakoshima, T. (2007). Structural basis for tubulin recognition by cytoplasmic linker protein 170 and its autoinhibition. Proceedings of the National Academy of Sciences *104*, 10346-10351.

Miyoshi, Y., Nagase, H., Ando, H., Horii, A., Ichii, S., Nakatsuru, S., Aoki, T., Miki, Y., Mori, T., and Nakamura, Y. (1992). Somatic mutations of the *APC* gene in colorectal tumors: mutation cluster region in the *APC* gene. Human Molecular Genetics *1*, 229-233.

Monshausen, G. B. and Gilroy, S. (2009). Feeling green: mechanosensing in plants. Trends in Cell Biology *19*, 228-235.

Monshausen, G. B. and Haswell, E. S. (2013). A force of nature: molecular mechanisms of mechanoperception in plants. Journal of Experimental Botany *64*, 4663-4680.

Mullen, J. L., Ishikawa, H., and Evans, M. L. (1998). Analysis of changes in relative elemental growth rate patterns in the elongation zone of *Arabidopsis* roots upon gravistimulation. Planta *206*, 598-603.

Muller, A., Guan, C., Galweiler, L., Tanzler, P., Parry, G., Bennett, M., Wisman, E., and Palme, K. (1998). *AtPIN2* defines a locus of *Arabidopsis* for root gravitropism control. The EMBO Journal *17*, 6903-6911.

Muller-Taubenberger, A. and Anderson, K. I. (2007). Recent advances using green and red fluorescent protein variants. Applied Microbiology and Biotechnology *77*, 1-12.

Mullis, K., Faloona, F., Scharf, F., Saiki, R., Horn, G., and Erlich, H. (1986). Specific enzymatic amplification of DNA in vitro: the polymerase chain reaction. Cold Spring Harbor symposia on Quantitative Biology *51*, 263-273.

Murashige, T. and Skoog, F. (1962). A revised medium for rapid growth and bio assays with tobacco tissue cultures. Physiologia Plantarum *15*, 473-497.

Nakagawa, Y., Katagiri, T., Shinozaki, K., Qi, Z., Tatsumi, H., Furuichi, T., Kishigami, A., Sokabe, M., Kojima, I., Sato, S., Kato, T., Tabata, S., Iida, K., Terashima, A., Nakano, M., Ikeda, M., Yamanaka, T., and Iida, H. (2007). Arabidopsis plasma membrane protein crucial for Ca^{2+} influx and touch sensing in roots. Proceedings of the National Academy of Science *104*, 3639-3644.

National Laboratory of Enteric Pathogens, Bureau of Microbiology, Laboratory Centre for Disease Control (1991). The polymerase chain reaction: an overview and development of diagnostic PCR protocols at the LCDC. The Canadian Journal of Infectious Diseases *2*, 89–91.

Nyabi, O., Naessens, M., Haigh, K., Gembarska, A., Goossens, S., Maetens, M., De Clercq, S., Drogat, B., Haenebalcke, L., Bartunkova, S., De Vos, I., De Craene, B., Karimi, M., Berx, G., Nagy, A., Hilson, P., Marine, J., and Haigh, J. J. (2009). Efficient mouse transgenesis using Gateway-compatible ROSA26 locus targeting vectors and F1 hybrid ES cells. Nucleic Acids Research *37*, e55. doi: 10.1093/nar/gkp112.

Obembe, O. O., Popoola, J. O., Leelavathi, S., and Reddy, S. V. (2011). Advances in plant molecular farming. Biotechnology Advances *29*, 210-222.

Okada, K. and Shimura, Y. (1990). Reversible root tip rotation in Arabidopsis seedlings induced by obstacle-touching stimulus. Science *250*, 274-276.

Perbal, G., Driss-Ecole, D., Tewinkel, M., and Volkmann, D. (1997). Statocyte polarity and gravisensitivity in seedling roots grown in microgravity. Planta *203*, S57-S62.

Pickett-Heaps, J. D. and Northcote, D. H. (1966). Organization of microtubules and endoplasmic reticulum during mitosis and cytokinesis in wheat meristems. Journal of Cell Science *1*, 109-120.

Pitzschke, A. and Hirt, H. (2010). New insights into an old story: *Agrobacterium*-induced tumour formation in plants by plant transformation. The EMBO Journal *29*, 1021-1032.

Powell, S. M., Zilz, N., Beazer-Barclay, Y., Bryan, T. M., Hamilton, S. R., Thibodeau, S. N., Vogelstein, B., and Kinzler, K. W. (1992). *APC* mutations occur early during colorectal tumorigenesis. Nature *359*, 235-237.

Prasher, D. C., Eckenrode, V. K., Ward, W. W., Prendergast, F. G., and Cormier, M. J. (1992). Primary structure of the *Aequorea victoria* green-fluorescent protein. Gene *111*, 229-233.

Prescott, M., Nowakowski, S., Nagley, P., and Devenish, R. J. (1999). The length of polypeptide linker affects the stability of green fluorescent protein fusion proteins. Analytical Biochemistry *273*, 305-307.

Rashotte, A. M., Brady, S. R., Reed, R. C., Ante, S. J., and Muday, G. K. (2000). Basipetal auxin transport is required for gravitropism in roots of *Arabidopsis*. Plant Physiology *122*, 481-490.

Rayle, D. L. and Cleland, R. E. (1992). The acid growth theory of auxin-induced cell elongation is alive and well. Plant Physiology *99*, 1271-1274.

Reddy, A. S. N. and Day, I. S. (2001). Kinesins in the Arabidopsis genome: a comparative analysis among eukaryotes. BioMed Central Genomics *2*:2. DOI: 10.1186/1471-2164-2-2.

Riechmann, J. L., Heard, J., Martin, G., Reuber, L., Jiang, C., Keddie, J., Adam, L., Pineda, O., Ratcliffe, O. J., Samaha, R. R., Creelman, R., Pilgrim, M., Broun, P., Zhang, J. Z., Ghandehari, D., Sherman, B. K., and Yu, G. (2000). *Arabidopsis* transcription factors: genome-wide comparative analysis among eukaryotes. Science *290*, 2105-2110.

Rogers, S. L., Wiedemann, U., Hacker, U., Turck, C., and Vale, R. D. (2004). *Drosophila* RhoGEF2 associates with microtubule plus ends in an EB1-dependent manner. Current Biology *14*, 1827-1833.

Roure, A., Rothbacher, U., Robin, F., Kalmar, E., Ferone, G., Lamy, C., Missero, C., Mueller, F., and Lemaire, P. (2007). A multicassette Gateway vector set for high throughput and comparative analyses in *Ciona* and vertebrate embryos. Public Library of Science ONE *2*, e916. doi:10.1371/journal.pone.0000916.

Sambrook, J., Fritsch, E. F., and Maniatis, T. (1989). Molecular cloning: a laboratory manual. Nolan, C. (ed.). 2nd edn. Plainview, NY: Cold Spring Harbor Laboratory Press.

Sanger, F., Nicklen, S., and Coulson, A. R. (1977). DNA sequencing with chain-terminating inhibitors. Proceedings of the National Academy of Sciences *74*, 5463-5467.

Schilperoort, R. A., Veldstraa, H., Warnaara, S. O., Muldera, G., and Cohena, J. A. (1967). Formation of complexes between DNA isolated from tobacco crown gall tumours and RNA complementary to *Agrobacterium tumefaciens* DNA. Biochimica et Biophysica Acta *145*, 523-525.

Schober, J. M., Cain, J. M., Komarova, Y. A., and Borisy, G. G. (2009). Migration and actin protrusion in melanoma cells are regulated by EB1 protein. Cancer Letters *284*, 30-36.

Shahidi, S. (2013). The microtubule-associated protein END BINDING 1 modulates membrane tracking pathways in plant root cells. Thesis for Degree of Master of Science. Simon Fraser University.

Shimomura, O., Johnson, F. H., and Saiga, Y. (1962). Extraction, purification and properties of aequorin, a bioluminescent protein from the luminous hydromedusan, *Aequorea.* Journal of Cellular and Comparative Physiology *59*, 223-239.

Skube, S. B., Chaverri, J. M., and Goodson, H. V. (2010). Effect of GFP tags on the localization of EB1 and EB1 fragments *in vivo*. Cytoskeleton *67*, 1-12.

Slep, K. C. (2010). Structural and mechanistic insights into microtubule end-binding proteins. Current Opinion in Cell Biology *22*, 88-95.

Slep, K. C., Rogers, S. L., Elliott, S. L., Ohkura, H., Kolodziej, P. A., and Vale, R. D. (2005). Structural determinants for EB1-mediated recruitment of APC and spectraplakins to the microtubule plus end. The Journal of Cell Biology *168*, 587-598.

Smith, E. F. and Townsend, C. O. (1907). A plant-tumor of bacterial origin. Science *25,* 671-673.

Smith, H. O. and Welcox, K. W. (1970). A restriction enzyme from *Hemophilus influenzae*: I. purification and general properties. Journal of Molecular Biology *51*, 379-391.

Smith, L. M., Sanders, J. Z., Kaiser, R. J., Hughes, P., Dodd, C., Connell, C. R., Heiner, C., Kent, S. B. H., and Hood, L. E. (1986). Fluorescence detection in automated DNA sequence analysis. Nature *321*, 674-679.

Squires, S. (2013). The microtubule-associated protein END BINDING 1b, auxin, and root responses to mechanical cues. Thesis for Degree of Master of Science. Simon Fraser University.

Squires, S. and Bisgrove, S. (2013). The microtubule-associated protein END BINDING1b, auxin, and root responses to mechanical cues. Journal of Plant Growth Regulation *32*, 681-691.

Staehelin, L. A. and Hepler, P. K. (1996). Cytokinesis in higher plants. Cell *84*, 821-824.

Stanga, J. P., Boonsirichai, K., Sedbrook, J. C., Otegui, M. S., and Masson, P. H. (2009). Statocyte polarity and gravisensitivity in seedling roots grown in microgravity. Plant Physiology *149*, 1896-1905.

Staves, M. P. (1997). Cytoplasmic streaming and gravity sensing in *Chara* intermodal cells. Planta *203*, S79-S84.

Stewart, C. N. Jr. (2001). The utility of green fluorescent protein in transgenic plants. Plant Cell Reports *20*, 376-382.

Su, L. K., Burrell, M., Hill, D. E., Gyuris, J., Brent, R., Wiltshire, R., Trent, J., Vogelstein, B., and Kinzler, K. W. (1995). APC binds to the novel protein EB1. Cancer Research *55*, 2972-2977.

Sugimoto, K., Himmelspach, R., Williamson, R. E., and Wasteneys, G. O. (2003). Mutation or drug-dependent microtubule disruption causes radial swelling without altering parallel cellulose microfibril deposition in *Arabidopsis* root cells. American Society of Plant Biologists *15*, 1414-1429.

Swarup, R., Kramer, E. M., Perry, P., Knox, K., Leyser, H. M. O., Haseloff, J., Beemster, G. T. S., Bhalerao, R., and Bennett, M. J. (2005). Root gravitropism requires lateral root cap and epidermal cells for transport and response to a mobile auxin signal. Nature Cell Biology *7*, 1057- 1065.

The Arabidopsis Genome Initiative (2000). Analysis of the genome sequence of the flowering plant *Arabidopsis thaliana.* Nature *408,* 796-815.

Thitamadee, S., Tuchihara, K., and Hashimoto, T. (2002). Microtubule basis for left-handed helical growth in Arabidopsis. Nature *417*, 193-196.

Tirnauer, J. S. and Bierer, B. E. (2000). EB1 proteins regulate microtubule dynamics, cell polarity, and chromosome stability. The Journal of Cell Biology *149*, 761-766.

Valentine, L. (2003). *Agrobacterium tumefaciens* and the plant: the David and Goliath of modern genetics. Plant Physiology *133*, 948-955.

Van Damme, D., Van Poucke, K., Boutant, E., Ritzenthaler, C., Inze, D., and Geelen, D. (2004). *In vivo* dynamics and differential microtubule-binding activities of MAP65 proteins. Plant Physiology *136*, 3956-3967.

Vaughan, K. T. (2005). TIP maker and TIP marker; EB1 as a master controller of microtubule plus ends. The Journal of Cell Biology *171*, 197-200.

Vaughn, L. M., Baldwin, K. L., Jia, G., Verdonk, J. C., Strophm, A. K., and Masson, P. H. (2011). The cytoskeleton and root growth behaviour, in Liu, B. (ed.). The plant cytoskeleton, advances in plant biology 2. New York, NY: Springer, 307-326.

Vincent, J. M. (1985). A manual for the practical study of root-nodule bacteria. Oxford, United Kingdom: Blackwell Scientific.

Vitre, B., Coquelle, F. M., Heichette, C., Garnier, C., Chretien, D., and Arnal, I. (2008). EB1 regulates microtubule dynamics and tubulin sheet closure *in vitro*. Nature Cell Biology *10*, 415-421.

von Arnim, A. G., Deng, X., and Stacey, M. G. (1998). Cloning vectors for the expression of green fluorescent protein fusion proteins in transgenic plants. Gene *221*, 35-43.

von Lintig, J., Kreusch, D., and Schroder, J. (1994). Opine-regulated promoters and LysR-type regulators in the nopaline (*noc*) and octopine (*occ*) catabolic regions of Ti plasmids of *Agrobacterium tumefaciens.* Journal of Bacteriology *176*, 495-503.

Wang, K., Herrera-Estrella, L., Van Montagu, M., and Zambryski, P. (1984). Right 25 bp terminus sequence of the nopaline T-DNA is essential for and determines direction of DNA transfer from *Agrobacterium* to the plant genome. Cell *38*, 455-462.

Ward, B. M. and Moss, B. (2001). Visualization of intracellular movement of vaccinia virus virions containing a green fluorescent protein-B5R membrane protein chimera. Journal of Virology *75*, 4802-4813.

Weisbrich, A., Honnappa, S., Jaussi, R., Okhrimenko, O., Frey, D., Jelesarov, I., Akhmanova, A., and Steinmetz, M. O. (2007). Structure-function relationship of CAP-Gly domains. Nature Structural and Molecular Biology *14*, 959-967.

Whittington, A. T., Vugrek, O., Wei, K. J., Hasenbein, N. G., Sugimoto, K., Rashbrooke, M. C., and Wasteneys, G. O. (2001). MOR1 is essential for organizing cortical microtubules in plants. Nature *411*, 610-613.

Wilms, F. H., Wolters-Arts, A. M., and Derkson, J. (1990). Orientation of cellulose microfibrils in cortical cells of tobacco explants: Effects of microtubule-depolymerizing drugs. Planta *182*, 1-8.

Wisniewska, J., Xu, J., Seifertova, D., Brewer, P. B., Ruzicka, K., Blilou, I., Rouquie, D., Benkova, E., Scheres, B., and Friml, J. (2006). Polar PIN localization directs auxin flow in plants. Science *312*, 883.

Wurch, T., Lestienne, F., and Pauwels, P. J. (1998). A modified overlap extension PCR method to create chimeric genes in the absence of restriction enzymes. Biotechnology Techniques *12*, 653-657.

Yadav, N., Vanderleyden, J., Bennett, D., Barnes, W., and Chilton, M-D. (1982). Short direct repeats flank the T-DNA on a Ti plasmid. Proceedings of the National Academy of Sciences *79*, 6322-6326.

Young, L. M., Evans, M. L., and Hertel, R. (1990). Correlations between gravitropic curvature and auxin movement across gravistimulated roots of *Zea mays*. Plant Physiology *92*, 792-796.

Zaenen, I., van Larebeke, N., Teuchy, H., van Montagu, M., and Schell, J. (1974). Supercoiled circular DNA in crown-gall inducing *Agrobacterium* strains. Journal of Molecular Biology *86*, 109-127.

Zale, J. M., Agarwal, S., and Loar, S. (2009). Evidence for stable transformation of wheat by floral dip in *Agrobacterium tumefaciens*. Plant Cell Reports *28*, 903-913.

Zhu, J., Oger, P. M., Schrammeijer, B., Hooykaas, P. J. J., Farrand, S. K., and Winans, S. C. (2000). The bases of crown gall tumorigenesis. Journal of Bacteriology *182*, 3885-3895.

Zupan, J., Muth, T. R., Draper, O., and Zambryski, P. (2000). The transfer of DNA from *Agrobacterium tumefaciens* into plants: a feast of fundamental insights. The Plant Journal *23*, 11-28.

Appendix A

Table A1 **Isolation of transgenic lines homozygous for single or multiple closely linked transgenes**

Truncation type	Generation T_1				Generation T_2
	Transformed lines	Observed number of hyg^R : hyg^S seedlings	Expected number of seedlings in 3 hyg^R : 1 hyg^S	p-value	Number of 100% hyg^R seed populations (number of populations tested)
EB1bΔC1	T1-1	528:20	411:137	<0.0001	N/A
	T1-2	455:8	347:116	<0.0001	
	T1-3	415:53	351:117	<0.0001	
	T1-4	685:11	522:174	<0.0001	
	T1-5	283:121	303:101	0.0216	
	T1-6	386:213	499:150	<0.0001	
	T1-7	269:22	218:73	<0.0001	
	T1-8	189:73	197:65	0.3000	1 (3)
	T1-9	226:63	217:72	0.2215	2 (2)
	T1-10	143:62	154:51	0.0760	In progress**
	T1-11	135:44	134:45	0.8630	2 (4)
EB1b[ΔC1]-GFP	T1-1	248:77	244:81	0.6084	in progress**
	T1-2	194:63	193:64	0.8855	in progress**
	T1-3	289:81	278:93	0.1580	in progress**
EB1bΔC2	T1-1	96:37	100:33	0.4231	1 (6)*
	T1-3	96:24	90:30	0.2059	4 (6)*
	T1-4	103:8	83:28	<0.0001	N/A
	T1-5	114:35	112:37	0.7051	3 (8)*
	T1-6	24:9	25:8	0.6877	0 (8)
	T1-8	98:27	94:31	0.4087	2 (6)
	T1-10	7:5	9:3	0.1824	1 (6)
	T1-11	23:12	26:9	0.2046	0 (6)

Truncation type	Generation T_1				Generation T_2
	Transformed lines	Observed number of hyg^R : hyg^S seedlings	Expected number of seedlings in 3 hyg^R : 1 hyg^S	p-value	Number of 100% hyg^R seed populations (number of populations tested)
EB1b[ΔC2]-GFP	T1-18	209:60	202:67	0.3243	in progress**
	T1-19	217:63	210:70	0.3340	in progress**
	T1-20	209:65	206:69	0.5984	in progress**
EB1bΔN	T1-2	83:39	92:31	0.0841	3 (5)
	T1-4	552:182	551:184	0.8779	in progress**
	T1-5	231:231	347:116	<0.0001	N/A
	T1-6	593:189	589:196	0.5640	in progress**
	T1-7	278:91	277:92	0.9043	in progress**
EB1b[ΔN]-GFP	T1-4	137:43	135:45	0.7306	in progress**
	T1-6	67:27	71:24	0.4348	in progress**
	T1-10	40:45	64:21	<0.0001	N/A
	T1-12	31:11	32:11	0.8586	in progress**

*Three lines were carried forward in the EB1bΔC2 root analysis: T1-1, T1-3, and T1-5. These lines are designated as EB1bΔC2 L1, L2, and L3, respectively. ** Genetic screening of transgenic plants has been passed on to Hae Ryoung Kim, the student who will continue with this project. N/A = non-applicable (These lines did not show evidence of a single transgene insertion site, thus looking for homozygosity was not applicable).